Absorption rates of carbon dioxide in amines in hydrophilic and hydrophobic solvents

Aravind V. Rayer, Paul D. Mobley, Mustapha Soukri, Thomas R. Gohndrone, Jak Tanthana, Jim Zhou, Marty Lail*

RTI International, 3040 Cornwallis Road, Durham, North Carolina, 27709

Abstract

The rate of absorption of CO_2 into amines in hydrophilic and hydrophobic solvent mixtures was studied in this work using a stopped-flow apparatus and a stirred-tank reactor. Monoethanolamine (MEA, primary amine) and N-methyl benzylamine (NMBZA, aromatic secondary amine) are chosen for this study and diluted in hydrophobic or hydrophilic solvents at different temperatures (295-343 K) and concentrations (0.01-4 $kmol.m^{-3}$). It was found that the reaction rate between the secondary amine and CO_2 in water is faster than the reaction with the linear primary amine (MEA); however, in an ethereal hydrophobic non-aqueous system the NMBZA-CO_2 reaction is slower than the reaction of CO_2 with MEA. With respect to amine, the reaction orders were found to be 0.9 and 1.2 for hydrophilic systems (MEA + H_2O, NMBZA + H_2O). For hydrophobic system they were found to be 0.6 and 2.7 (NMBZA + ethereal hydrophobic solvent, NMBZA + MePhOH + ethereal hydrophobic solvent). When amine was mixed with hydrophilic solvent (H_2O), the activation energy of amine (NMBZA) to react with CO_2 was found to be 27.66 $kJ.mol^{-1}$ and decreased to 10.37 $kJ.mol^{-1}$ when mixed with hydrophobic solvent (ethereal hydrophobic solvent). The activation energy of hydrophobic solvent was found to increase by adding an alcohol to the solvent (MePhOH + ethereal

hydrophobic solvent). Both the zwitterion and termolecular mechanism were applied to the experimental data. It was found that deprotonation of the zwitterion and deprotonation of the loosely bound complex was the rate limiting step for the zwitterion and termolecular mechanism, respectively.

Additionally, activators such as water, piperazine (PZ), and 4-hydroxy piperidinol (HPIP) were added to the ethereal hydrophobic non-aqueous solvent to determine the effect on the reaction rate. It was found that the water- and amine-based activators lead to an increase in the observed reaction rates as the concentration of the activators increased. The reaction of NMBA with CO_2 and PZ exhibited a higher reaction rate but the PZ was insoluble in the non-aqueous NMBZA system, whereas HPIP remained soluble and offered a similar reaction rate. The activation energy of ethereal hydrophobic non-aqueous solvent to react with CO_2 increased from 27.98 to 32.83 $kJ.mol^{-1}$ by adding PZ and 33.51 $kJ.mol^{-1}$ by HPIP and remained by adding H_2O (26.78 $kJ.mol^{-1}$). From this work, it was found that the non-aqueous solvent plays an important role in the reaction rate of CO_2 with amines. Activators and solvents can be selected to increase the reaction rate with CO_2.

1. Introduction

Improving the efficiency of gas-liquid absorption systems for large-scale Carbon Capture and Sequestration (CCS) in the power sector as well as other industrial sectors with high CO_2 emissions remains a technological challenge that can still be improved to be more energy efficient. Current available large scale technologies used to minimize the post-combustion CO_2 emissions from fossil fuel-fired power plants or other large-scale industrial point sources such as cement or steel plants are currently accompanied with a high cost in terms of the energy required to separate CO_2, which is referred to as the parasitic energy load or penalty [1]. To reduce the power deficit and associated cost for this parasitic energy, advanced solvents are being developed around the world.

Thermal swing regeneration of solvents is the most practiced method for a conventional carbon capture process. An ideal solvent is one that exhibits high CO_2 absorption capacity, fast reaction rate, low cost, low corrosivity, high thermal and chemical stability, low vapor pressure, and low regeneration heat duty [2]. The amount of heat input needed to release the CO_2 reacted with the amine is dependent on the sensible heat, the heat of vaporization and the heat of reaction s [3]. As mentioned by the comprehensive review of solvent-based post-combustion CO_2 capture processes [4], several chemical solvents have been screened to determine an optimized novel solvent with all the required properties to reduce the cost of CO_2 capture. Lail et al. [5] proposed a non-aqueous solvent by considering the three terms in equation 1. This led to a designed solvent with lower sensible heat, lower vapor pressure and lower heat of absorption with higher CO2 working capacity compared to previously studied amines systems. The solvent improvements can reduce the reboiler duty required for CO2 capture to 2.0 GJ/kg_{CO2}, which results in a ~55% reduction compared to the industrial standard aqueous 30wt% MEA solvent

(3.75 GJ/kgCO2) [5]. Lail et al. [5] used a hydrophobic, non-aqueous, organic component that decreased the sensible heat requirement in the process due to the decreased heat capacity compared to traditional aqueous systems. In this work the reaction rate between the non-aqueous amines and CO_2 was measured to further characterize their use for a CO_2 capture process.

The capital cost is important to consider in addition to the energy requirement of a thermal-swing process. The overall acid gas absorption rate and the design of absorption column depend on the rate of reaction between amines in different reaction media and CO_2. A solvent with faster kinetics will require a shorter, smaller absorber column and thus decrease the cost of the construction materials of the capture process. Hence, there is a need for a thorough understanding of the reaction mechanism in different media and the corresponding reaction rate constants. Since 1960, the reaction kinetic data for aqueous primary, secondary, and tertiary amines with CO_2 has been published and reviewed by various researchers [6]. Although aqueous systems are the most prevalent in literature, the reaction kinetics of CO_2 with amines in non-aqueous solvents has also been studied to design an optimum solvent with lower vapor pressure, lower heat capacities, and faster reaction rates.

Recently, reversible guanidine compounds and $_{CO2}$-binding organic liquids were proposed to post-combustion CO_2 capture and found to have high boiling points, low vapor pressures, good physical and chemical absorption capacities, lower heat capacities, and limited reaction rates with non-corrosive nature [7],[8],[9]. The reaction rates of non-aqueous systems could be increased by the use of promoters [10]. Attempt of adding alkanol components in non-aqueous solvents to increase its reaction rates found to be little effect [11]. Solubility of the activators in non-aqueous solvents hinders the ability to promote reaction rate with CO_2 and limits the quantity of activators [12]. In this work, we are exploring the effect of activators which are

soluble (HPIP) and insoluble (PZ) in non-aqueous solvents to improve the reaction rate CO_2 with non-aqueous solvent having low reaction enthalpy.

Promising non-aqueous solvents studied in the literature to determine the reaction rate with CO_2 are given in given in Supplemental Information (Table 11). The most commonly studied non-aqueous diluents are alcohols and glycols due to the amine solubility. Non-aqueous solvent developed in Research Triangle Institute (RTI) with hydrophobic amines and hydrophobic organic solvents showed an impactful increment in the CO_2 absorption capacity and reduction in regenerating energy in CO_2 capture by minimizing the amount of water and reducing the hydrogen bonding that increases the stability of CO_2-amine complex [3].Moreover less polar hydrophobic solvents would not stabilize the carbamic acid through hydrogen bonding and would promote the carbamate formation[13]. In this work, a secondary amine, N-methyl benzylamine, is mixed with 4-methoxy phenol and polyethylene glycols. Each of the components is chosen based on their hydrophobicity. The NMBZA is a secondary amine with a hydrophobic aromatic functional group, the phenol is also aromatic leading to hydrophobic mixture properties, and the polyethylene glycols are chosen as the diluent based on their low vapor pressure and low water solubility. Solvent mixtures of these components were studied to determine the reaction rate of the amine with CO_2 at different temperatures and concentrations.

Benzylamine (BZA) functional group, one of the only examples of an amine with an aromatic substituent in literature, possesses a high CO_2 absorption rate when considered as a constituent of an aminosilane [14]. BZA has many advantages such as readily biodegradable [15], lower corrosion rate and oxidative degradation compared to MEA [16], and a low vapor pressure and boiling point comparable to MEA [17, 18]. Though most of the benzene-based chemicals are carcinogenic, BZA is not listed as a carcinogen by the International Agency for

research on Cancer and it has a National Fire Protection Association rating similar to MEA with a flash point of 338 K [19]. Aqueous BZA has lower viscosity and heat capacity compared to aqueous MEA with high thermal and oxidative stability [19]. In spite of the beneficial properties of the BZA functional group, there has not been any further attempts to improve the reaction rate of CO_2 with additional benzene-substituted amine molecules for PCC. Richner et al. [19] studied the reaction kinetics of CO_2 with BZA at temperatures 288-318 K and reported the reaction kinetics similar to that of aqueous MEA. BZA was found to have a larger enthalpy of protonation resulting in a larger temperature dependent change in basicity and enhanced the CO_2 cyclic capacity [19]. They concluded that the major disadvantage of BZA is the formation of a precipitate at high concentrations of BZA upon absorption of CO_2. In this work, a benzene substituted amine in the family of BZA (i.e., N-methyl benzyl amine, NMBZA [20]) was chosen as the reactive component in aqueous and non-aqueous solvents for evaluating its reaction rates with CO_2.

Widely used stopped-flow apparatus and a stirred-tank reactor were utilized to study the reaction kinetics of CO_2 with NMBZA in water (0.52-3.97 kmol.m^{-3}) and NMBZA in ethereal hydrophobic solvents (i.e., in tetra ethylene glycol dibutyl ether and polyethylene glycol dibutyl ether (Genosorb 1843)) with a concentration range of 0.01-4 kmol.m^{-3} at a temperature range of 295-353 K. When dealing with reactions with varying overall reaction order the order and reaction rate constant depends on the concentration range. Stopped flow in this work is a homogeneous rapid mixing method and requires low concentration while heterogenous Gas-Liquid absorption using stirred cell requires high concentration [21]. Additionally, the modified stopped-flow apparatus for high-temperature was used to measure the unreported data for the reaction kinetics of aqueous MEA with a concentration range of 0.01-0.1 kmol.m^{-3} at a

temperature range of 298-353 K. Obtained results were fitted with a well-known proposed mechanism for reaction of CO_2 with amines in aqueous and non-aqueous solvents.

2. Theoretical Background

The reaction rate experiments are modeled using the commonly described mechanisms for the reaction between CO_2 and highly reactive amines. The two mechanisms are the zwitterion mechanism, which was proposed by Caplow in 1968 [22] and reintroduced by Danckwerts in 1979 [23], and the termolecular mechanism, which was proposed by Crooks and Donnellan in 1989 [24].

2.1. Zwitterionic mechanism

The formation of a zwitterion followed by deprotonation of the zwitterion by a base are the main two steps involved in zwitterion mechanism as proposed by Caplow[22]. The base that deprotonates the zwitterion can be either water or a second mole of the amine. This mechanism explains first, second and fractional order reaction kinetics for a variety of amines in aqueous and non-aqueous solvents.

For these mechanisms, the overall forward reaction rate derived with the assumption of a quasi-steady state condition for the zwitterionic concentration is given by:

Equation 1:r ———————

Where is the forward second order reaction rate constant ($m^3.mol^{-1}.s^{-1}$) for the Zwitterion mechanism; k_{-1} is the backward first order reaction rate constant (s^{-1}); is the contribution to the removal of the proton by all bases present in the solution; and k_B and k_{-B} are the forward and backward second order reaction rate constants for base B ($m^3.mol^{-1}s^{-1}$). There are two asymptotic situations that exist for Equation 1. When the second term in the denominator is <<1,

the overall reaction rate expression is reduced to second-order indicating almost all of the zwitterion is deprotonated before it reverts to amine and CO_2 as follows:

Equation 2:r

The rate-determining step for the above reaction is the formation of the zwitterion which is not catalyzed by any base in the solution. When the second term in the denominator in Equation 1 is >>1, the overall reaction becomes:

Equation 3:r ———————

The overall order of reaction is three, indicating that there is some Brønsted effect taking place with bases in the solution that prevents the deprotonation of the zwitterion. This may be due to lower basicity of bases, or steric hindrance of the lone pair of the nitrogen atom inhibiting the interaction and removal the proton in the zwitterion. Therefore, the deprotonation of the zwitterion is the rate-determining step in this reaction. In the case of aqueous solutions, the water, OH- ions, and the amine act as bases, while in the non-aqueous case, only the amine is regarded as a base.

2.2. Termolecular mechanism

Crooks and Donnellan[24] concluded that the reaction of CO_2 with highly reactive amines is via a single-step reaction that forms a loosely bound encounter complex as an intermediate. The proton transfer and the bonding between amine and CO_2 take place simultaneously as follows:

If any one of the bases in the solvent is dominate in the contribution to deprotonation of the zwitterion or loosely bounded complex, then both Equation 1 and Equation 3 will be reduced to a form as below [25]:

Equation 4:r _____

Where, dB is the dominating base or component in the solvent. In an aqueous solvent system with a low amine concentration, the dominating base deprotonating the zwitterion may be water, but with a higher amine concentration, the dominating base may be the amine *(k_2^Z or k_2^T).* In a non-aqueous solvent system with a low amine concentration, the deprotonating ability of the amine (k_2^T) may be hindered by the non-aqueous diluent in the solvent. But the contribution of bases or components may vary for different system and temperatures.

In this work Equation 1, Equation 2, Equation 3 or Equation 4 were used to correlate the experimental data in accordance with the obtained reaction order with respect to amine. The equation with the best AAD% (Percentile absolute average deviation) was chosen to interpret the mechanism of reaction.

3. Experimental Details

Reagents used in this work were obtained from Sigma-Aldrich with a mass purity of 97-99.5% and their hydrophobicity and molecular structure are shown in Table 1.All the chemicals were used without further purification. In this work, two experimental set-ups were used to obtain the pseudo first-order reaction kinetics for aqueous and non-aqueous solvents. The first system that was studied in a stop-flow apparatus is aqueous MEA to compare with the literature results. The second system studied is the hydrophobic NMBZA + TEGDBE with and without

water. One final system was studied in the stirred tank setup where the diluent was changed from the TEGDBE to the commercially available Genosorb 1843 (Clariant) [26]. Genosorb 1843 has a lower molecular weight than TEGDBE but is similar in structure and properties. In addition, phenol was added to minimize the heat of absorption and included to determine the effect it has on the kinetics.

3.1. Stopped-flow apparatus

Figure 1 shows the schematic drawing of the experimental stopped-flow equipment (SF-51) with both a low and high temperature thermostat option purchased from Hi-Tech Scientific Ltd. (UK). It consists of six major parts: a sample handling unit, a conductivity detection cell, an A/D converter, a microprocessor with a computer, a water bath to control the temperature within ±0.1 K and a Temperature Pod (TPod) attached to the sample cell to thermostat the cell for high temperatures separately from the main water bath. The temperature range of this TPod can be controlled between -20ºC to 90ºC. Dimensions of the conductivity cell are 3 mm in length and 3 mm in diameter with platinum electrodes at each end. The nominal cell constant is 4.2 cm^{-1} and the deadtime of the reaction is 2.5 ms. One injection will fill the cell with 75 µl reagent from 5 ml sample syringes. Conductivity detection ranges are 0-0.0005 Siemens. During an experimental run, CO_2 saturated solvent is added to one sample syringe and a fresh sample of the reacting solvent is loaded in the second. The Kinetasyst software is used to actuate the pneumatically controlled drive plate which accurately injects the solution into the conductivity cell through a mixing loop. The rate of change of conductivity of the rapid homogenous reaction was monitored as a voltage signal and fit with the Kinetic Studio software. The conductivity change is measured as a function of time by a circuit described by Knipe et al. [27] and fit to an exponential equation resembling a first-order kinetic equation as:

Molecule Name	Nature	Molecular structure

Equation 5:

Where k_0 is the pseudo first-order reaction rate constant as the experiment is conducted under pseudo first-order conditions and *t* is the time of the injection in sec. For each run, a freshly saturated CO_2 solution is obtained by bubbling CO_2 gas through the desired solvent and then the saturated CO_2 solvent is diluted with the fresh amine/solvent formulation by injection with the two syringes to ensure that the reaction is in the pseudo-first order regime where an amine concentration in excess to that of CO_2 (i.e., mol_{amine} to mol_{CO2} is kept greater than 20) for all the experiments. The saturated concentration of CO_2 in solution was calculated using the Henry's constant of CO_2 in the solvent at room temperature. Experiments were repeated at least 7 times at each temperature for all the concentrations of solvents. The reproducibility for k0 was of 3 AAD%. Pseudo first-order rate constants of the aqueous solutions of MEA obtained in this work were compared with published data [28] in Figure 12. An estimated uncertainty of 5 AAD% was found when compared to published data for aqueous solutions of MEA. The uncertainty in preparing the desired concentration was found to be 0.05%. Using the stopped-flow apparatus the reaction kinetics of MEA + H_2O + CO_2 and NMBZA + H_2O + CO_2 with a concentration range of 0.01-0.1 $kmol.m^{-3}$ were studied and compared with literature of same concentrations and temperature ranges [28]. NMBZA + H_2O + TEGDBE with a concentration range of 0.025-1.9 $kmol.m^{-3}$ were studied at a temperature range of 298-353 K. The obtained results were correlated with the zwitterion and termolecular mechanisms.

Table 1. Molecular structure and hydrophobicity of studied molecules in this work

Monoethanolamine (CAS.No:141-43-5)	Hydrophilic	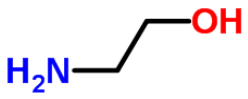
N-methyl benzylamine (CAS.No: 103-67-3)	Hydrophobic	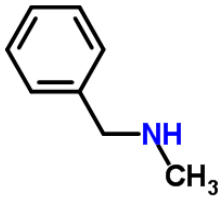
Water (CAS.No: 7732-18-5)		
TEGDBE (CAS.No: 112-98-1)	Hydrophobic	
MePhOH (CAS.No: 150-76-5)	Hydrophobic	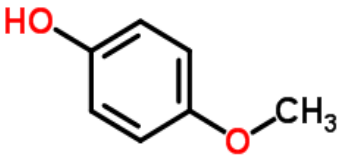
Genosorb 1843 (CAS.No: 31885-97-9)	Hydrophobic	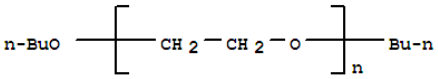
Piperazine (CAS.No:110-85-0)	Hydrophilic	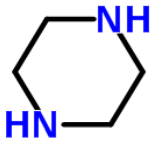
4-Hydroxypiperidinol (CAS.No:5382-16-1)	Hydrophilic	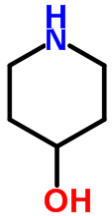

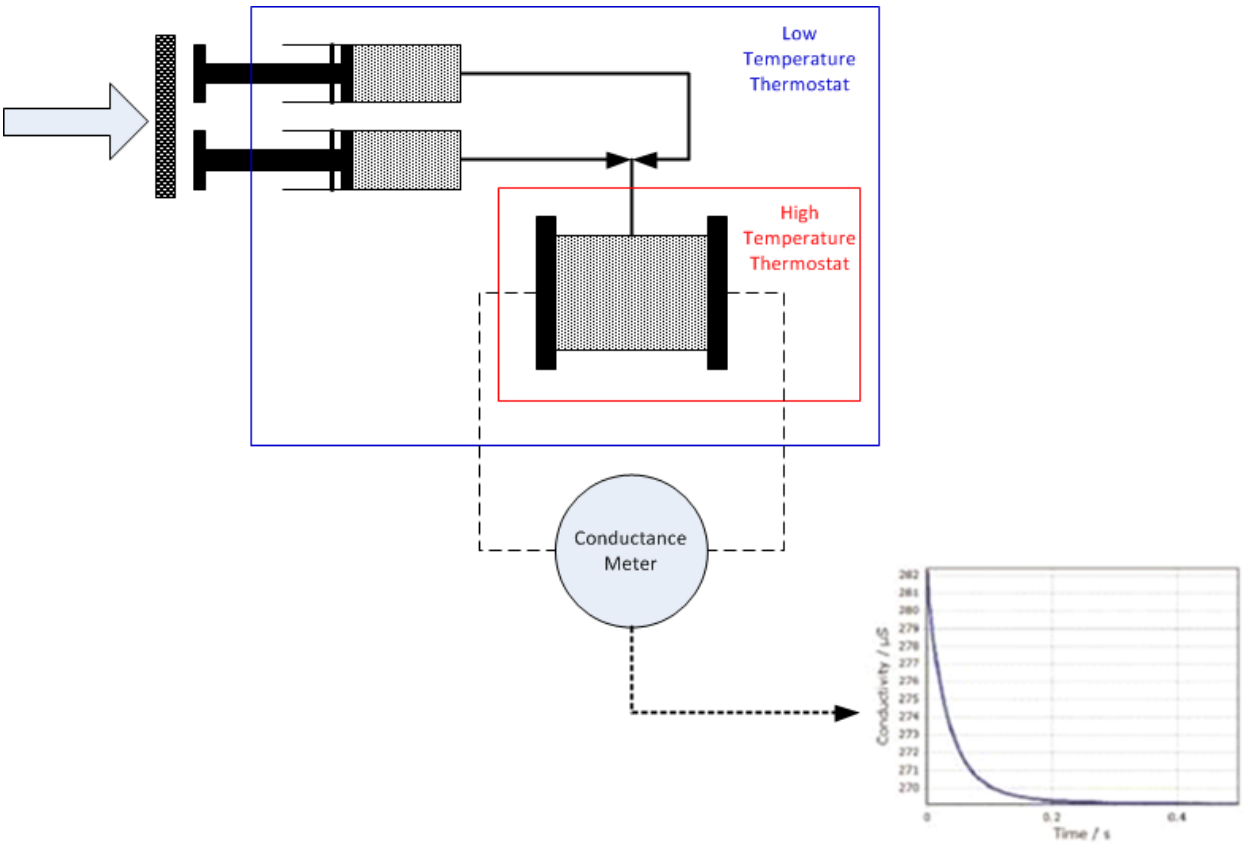

Figure 1. Schematic diagram of low and high temperature stopped-flow equipment

3.2. Stirred-tank reactor

Because of negligible conductivity in the mixture of NMBZA + MePhOH + Genosorb 1843, the stopped-flow apparatus was not able to determine the reaction rate of CO_2 in the mixture. Therefore, reaction rate of CO_2 with NMBZA + MePhOH + Genosorb 1843 was determined in a stirred-tank reactor in a calorimeter (Chemisens AB, Sweden) with an automated gas handling and monitoring system using the procedure suggested by Kierzkowska-Pawlak et al.[25]. The calorimeter is equipped with a fully automated and computer-controlled, stirred reactor vessel. A schematic diagram of the experimental set-up for the stirred-tank reactor is given in Figure 2. The reactor is a cylindrical glass vessel with 4 stainless steel baffles to maintain a horizontal gas-liquid interface. The cell contains stainless steel stirrers to agitate both

the liquid and gas phases. A propeller stirrer and a turbine stirrer with four blades was used for mixing the liquid and gas phase, respectively. The reactions are run under isothermal conditions where the temperature is maintained by a circulating heat transfer fluid (i.e., propylene glycol) through the base of the reactor. The reactor pressure is monitored by a pressure transducer mounted on the reactor with an accuracy of ± 0.03% of the full range of 35 kPa.

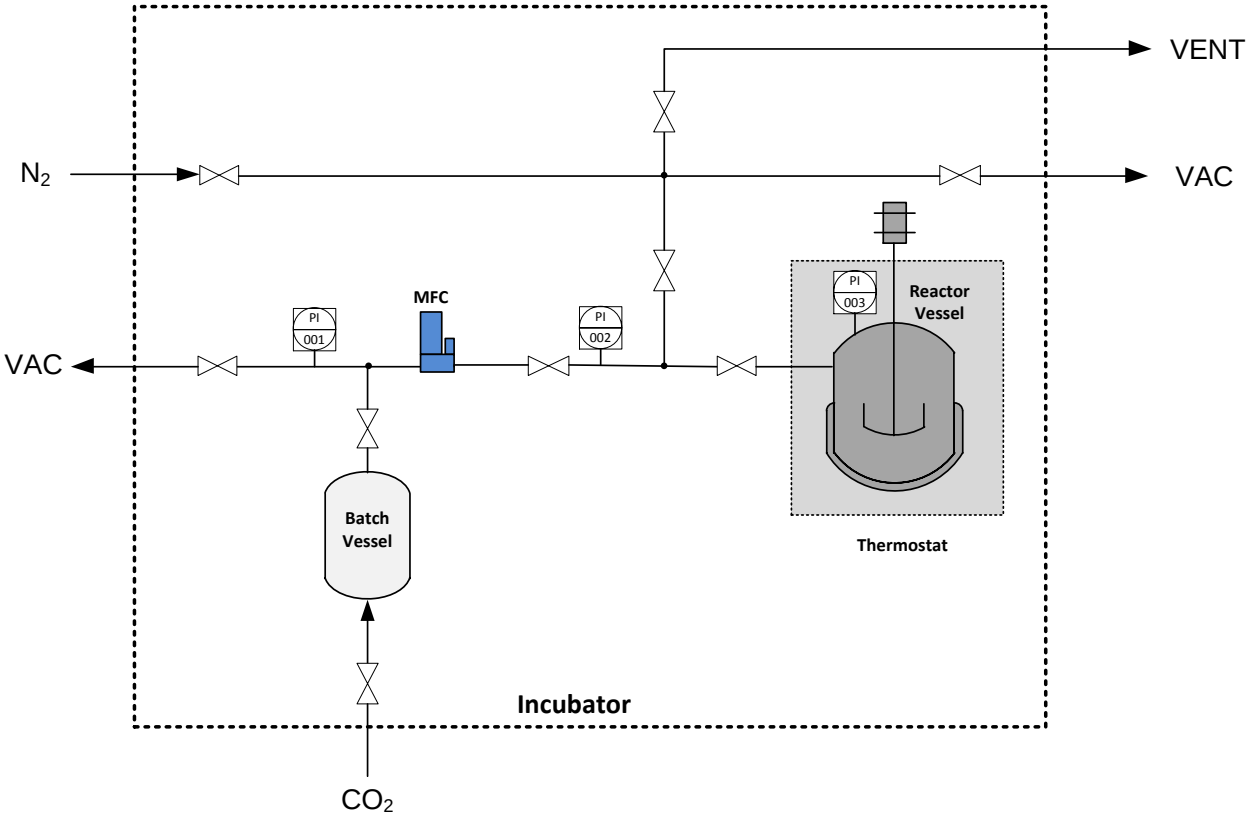

Figure 2. Schematic diagram of stirred-tank reactor

In each experiment, the reactor is loaded with 100 mL of fresh solvent. After loading, the cell is purged with N_2 and degassed using vacuum (~10 kPa) for 3 hours to ensure that any dissolved gases are removed from the system. While under vacuum, the stirrer is set to 500 rpm and the sample is given time to reach thermal equilibrium. When the temperature in the reactor becomes stable at the desired value, the stirring is stopped for a moment and pure CO_2 is introduced into

ACCEPTED MANUSCRIPT

the upper part of the reactor for a very short time. The initial pressure of the experiment is noted (~14-21 kPa). The initial pressure of the system is low to satisfy the criterion of a fast pseudo first order regime. Then the reactor is stirred at the desired speed (120-150 rpm) to maintain a flat interface and thus a constant liquid-gas reaction surface area.

The reduction in the reactor pressure due to the absorption of CO_2 is monitored by the pressure transducer. The partial pressure of CO_2 (P_{CO2}) is recorded as a function of time until the gas-liquid equilibrium is reached. Based on the P_{CO2} *vs time* data, the reaction rate of CO_2 with solvent is calculated. For a fast pseudo-first order, irreversible reaction, Kierzkowska-Pawlak et al. [25] derived an expression for a change in partial pressure of CO_2 with respect to time given as:

Equation 6:P

Where, P_{CO2} is the partial pressure of CO_2 (kPa); is the partial pressure of CO_2 at the start of absorption (t = 0); R is the universal gas constant (8.314 kPa.m^3.kmol^{-1}.K^{-1}); T is the experimental temperature; A is the interfacial area (2.26×10^{-3} m^2); V_G is the gas phase volume (m^3); H_{CO2} is the Henry's coefficient (kPa.m^3.kmol^{-1}); k_{ov} is the overall kinetic rate constant (s^{-1}); D_{CO2} is the diffusion coefficient of CO_2 in the solvent (m/s); and t is the experimental time. The fast pseudo-first order reaction regime without depletion of the amine at the gas-liquid interface was achieved by maintaining the following condition in each experiment:

Equation 7: $10 < Ha < E_{inf}$

Where Ha is the Hatta number, and E_{inf} is the enhancement factor for an irreversible instantaneous reaction, which are defined as:

Equation 8:Ha ——— *and* ———

Where, D_{NMBZA} is the diffusivity coefficient of NMBZA in the mixture; *[NMBZA]* is the concentration of NMBZA in NAS; ν_{NMBZA} is the reaction stoichiometric coefficient of amine content in NAS with CO_2; and *[CO_2]* is the concentration of CO_2. The physical properties required to calculate the reaction rate constant (i.e., densities, viscosities, Henry's constant, and diffusion coefficients of CO_2 in the solvent and diffusion coefficients of NMBZA in solvent at different temperatures and concentrations) were measured experimentally (listed in *Table 17. Experimental kinetic data for NMBZA + TEGDBE (hydrophobic) with different water, Pz, and HPIP concentrations at different temperatures from Stopped-flow apparatus*

Concentration ($kmol.m^{-3}$)	**Effect of concentration of water**			**Effect of concentration of Pz**			**Effect of concentration of water and Pz**	
[NMBZA]	**1.22**	**1.22**	**3.50**	**3.50**	**3.50**	**3.50**	**3.50**	**3.50**
Activators	**0.00**	**0.00**	**0.00**	***0.11***	***0.45***	***0.87***	***0.87***	***1.09***
[water]	**0.52**	**2.61**	**2.61**	**2.61**	**2.61**	**2.61**	**3.97**	**3.97**
[TEGDME]	**2.90**	**2.76**	**1.74**	**1.70**	**1.59**	**1.46**	**1.37**	**1.30**
T (K)	**Pseudo first-order rate constant (k_0)**							
298.15	481	526	888	941	1028	1169	1170	1170
303.15	749	820	1253	1316	1356	1398	1410	1560
308.15	951	1050	1438	1500	1575	1587	1657	1980
313.15	1056	1160	1582	1605	1819	1947	1879	2292
323.15	1149	1287	2300	2358	2500	2471	2544	3736
333.15	1252	1504	2964	3185	3387	3448	3558	5769
343.15	1772	2062	3861	3902	4473	4987	5421	7604
353.15	2510	2788	5312	5623	5923	6223	6884	8404

Table 18- Supplemental information) and estimated using standard available correlations such as the Wilke-Chang technique[29].

The experimental data obtained for aqueous AEEA (2-(2-aminoethylamino) ethanol) with a concentration of 2.5 kmol.m^{-3} from this work was compared with researchers who used a similar reactor setup (Kierzkowska-Pawlak et al.[25] and Mamun et al. [30]) and found to be within 5.6 AAD% and 10 AAD% as shown in Figure 13. Using this procedure, the overall reaction rates for CO_2 in the NMBZA + MePhOH + Genosorb 1843 mixture was measured in the concentration range of 0.7-3.5 kmol.m^{-3} and temperatures ranging from 295-353K.

4. Experimental Results and Discussion

4.1. Experimental Results

The reaction rates of CO_2 in both hydrophobic and hydrophilic systems were studied using the stopped-flow apparatus and a stirred-tank reactor at different concentrations and different temperatures. Table 2 reports the experimental conditions at which the reaction rates were measured for the hydrophobic systems. Table 12 shows the obtained pseudo first-order rate constants (k_0) at different concentrations and the rate constants are plotted in Figure 3-Figure 6. At each temperature, an empirical power law curve (k_0 = m *[Amine]^n), correlating the pseudo first-order rate constants (k_0) and amine concentrations gives a reaction order with respect to amine and the overall reaction order is the sum of orders of amine and CO_2. The calculated reaction order for the studied systems are given in Table 2. Reaction order with respect to amine less than unity indicates the hinderance of reaction with CO_2 by the presence of another component (TEGDBE) and reaction order greater than unity shows that the presence of another component enhances the reaction rate (MePhOH).[21]. To obtain this fractional order and 3rd order reaction as a function temperature and concentration of amines, an empirical model was developed from empirical power law and fitted to the reaction rate of CO_2 with the solvents and their reaction order at different temperatures with the following expression:

Equation 9: $k_0 = m * [Amine]^n = [(A$

Where, *[Amine]* concentration in *Equation 9* is in *mol.m*$^{-3}$; T_0 is the reference temperature of value 273K; and A, B, C, D and E are the fit coefficients of *Equation 9* and their values are given in *Table 3* along with their reaction order and R^2 values. The term *n* in Equation 9 is the reaction order $[n = (C * (T - T_0)^2 + D * (T - T_0) + E)]$. The zwitterion and termolecular

mechanisms were fit to the experimental rate data obtained in this work using *Equation 1, Equation 2, and Equation 3 or Equation 4*.

Table 4-Table 7 show the k_2 values obtained from the different mechanisms for all of the studied systems at different temperatures. The best fit mechanism and their corresponding AAD% are given in

Table 8 for all of the studied systems with their second order reaction rate constant (k_2) expressions to calculate the pseudo-first order reaction rate constants ($k_0 = k_2$ [Amine]). Parity plots for the best fit mechanism are given in Supplementary Information (*Figure 14-Figure 17*). The temperature dependent Arrhenius equation value of individual constants obtained for the proposed mechanisms are given as follows:

For (MEA + H_2O) system:

Equation 10: $k = 4.07 \quad exp(\frac{\quad}{\quad}$ $[R^2 = 0.99]$

Equation 11: $k = 2.3 \times 10^6 \, exp(\frac{\quad}{\quad}$ $[R^2 = 0.99]$

Equation 12:k = 1.51 10^5 exp (——— [R^2 = 0.99]

For (NMBZA + H_2O) system:

Equation 13:k = 1.46 × 10^5 exp (———[R^2 = 0.97]

Equation 14:k = 4.37 × 10^{27} exp (——— [R^2 = 0.99]

Equation 15:k = 2 .56 10^4 exp (——— [R^2 = 0.99]

For (NMBZA + H_2O +TEGDBE) system:

Equation 16:k = 6.77 × 10^1 exp (———)[R^2 = 0.92]

Equation 17:k = 1.47 × 10-1 exp (—— [R2 = 0.98]

Equation 18:k = 4.73 10^4 exp (——— [R^2 = 0.99]

For (NMBZA + MePhOH + Genosorb 1843) system:

Equation 19:k = 1.73 × 10^3 exp (———)[R^2 = 0.94]

Equation 20:k = 1.73 × 10^{-2} exp (——— [R^2 = 0.94]

Equation 21:k = 5.73 × 104 exp (——— [R2 = 0.96]

Table 2. Experimental conditions of this work and the calculated values of reaction

			[Amine]		Order of reaction (*n*)	
					w.r.t	
Studied System	Type	Equipment	*kmol.m*$^{-3}$	T/K	*amine*	*Overall*
MEA + H_2O	Hydrophillic	Stopped-flow	0.01-0.1	298-343	0.89 ~ 1	2
NMBZA + H_2O	Hydrophillic	Stopped-flow	0.01-0.1	298-344	1.23~1	2
NMBZA + H_2O + TEGDBE	Hydrophobic	Stopped-flow	0.025-1.9	298-345	0.58	1.58
AEEA + H_2O	Hydrophillic	Stirred-tank	2.5	295-353	--	--
NMBZA + MePhOH + Genosorb 1843	Hydrophobic	Stirred-tank	0.72-3.5	295-353	2.73	3.73

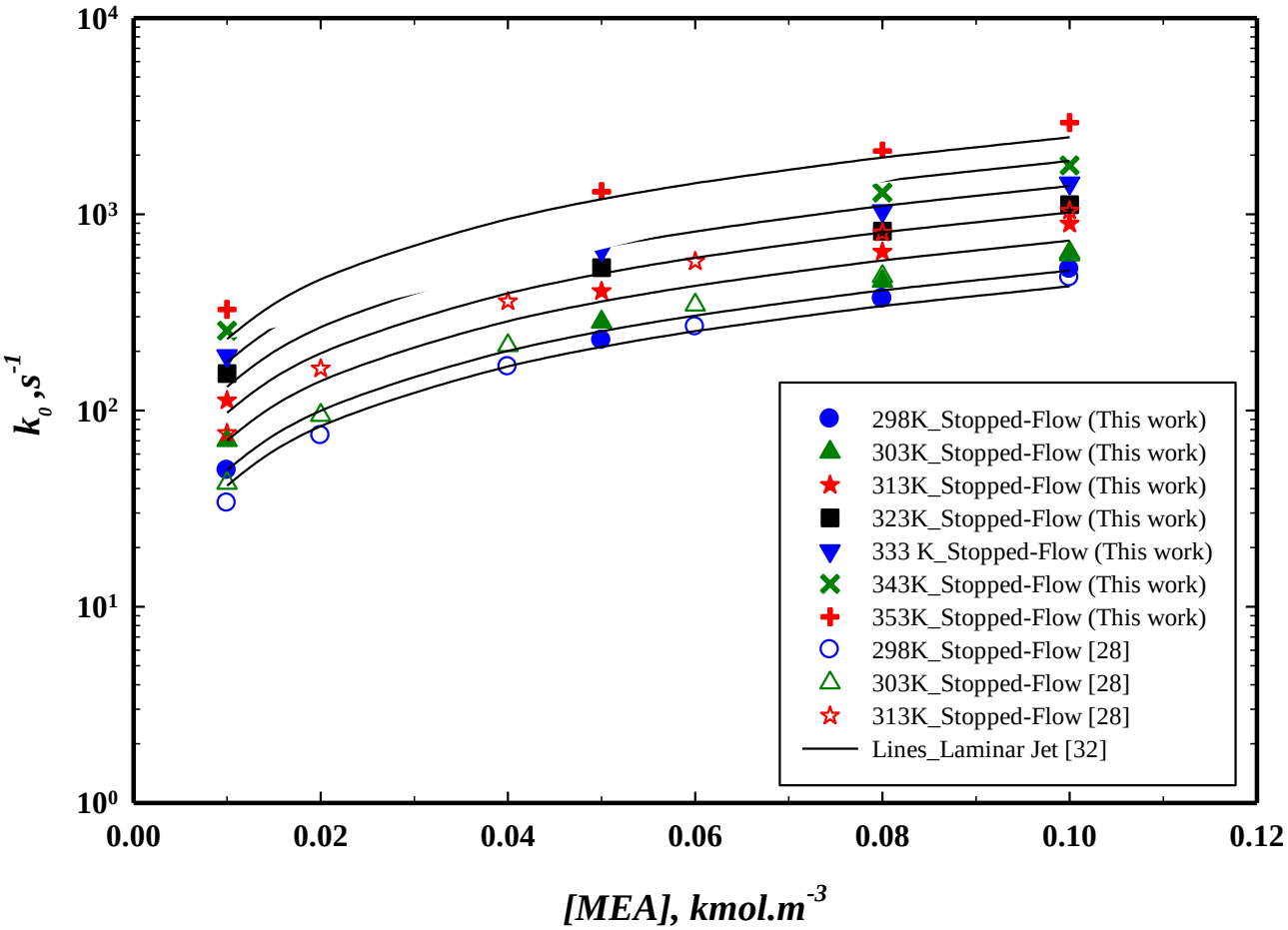

Figure 3. Comparison of measured and predicted reaction kinetics of aqueous MEA with CO_2 (hydrophilic system) at low concentrations using termolecular model

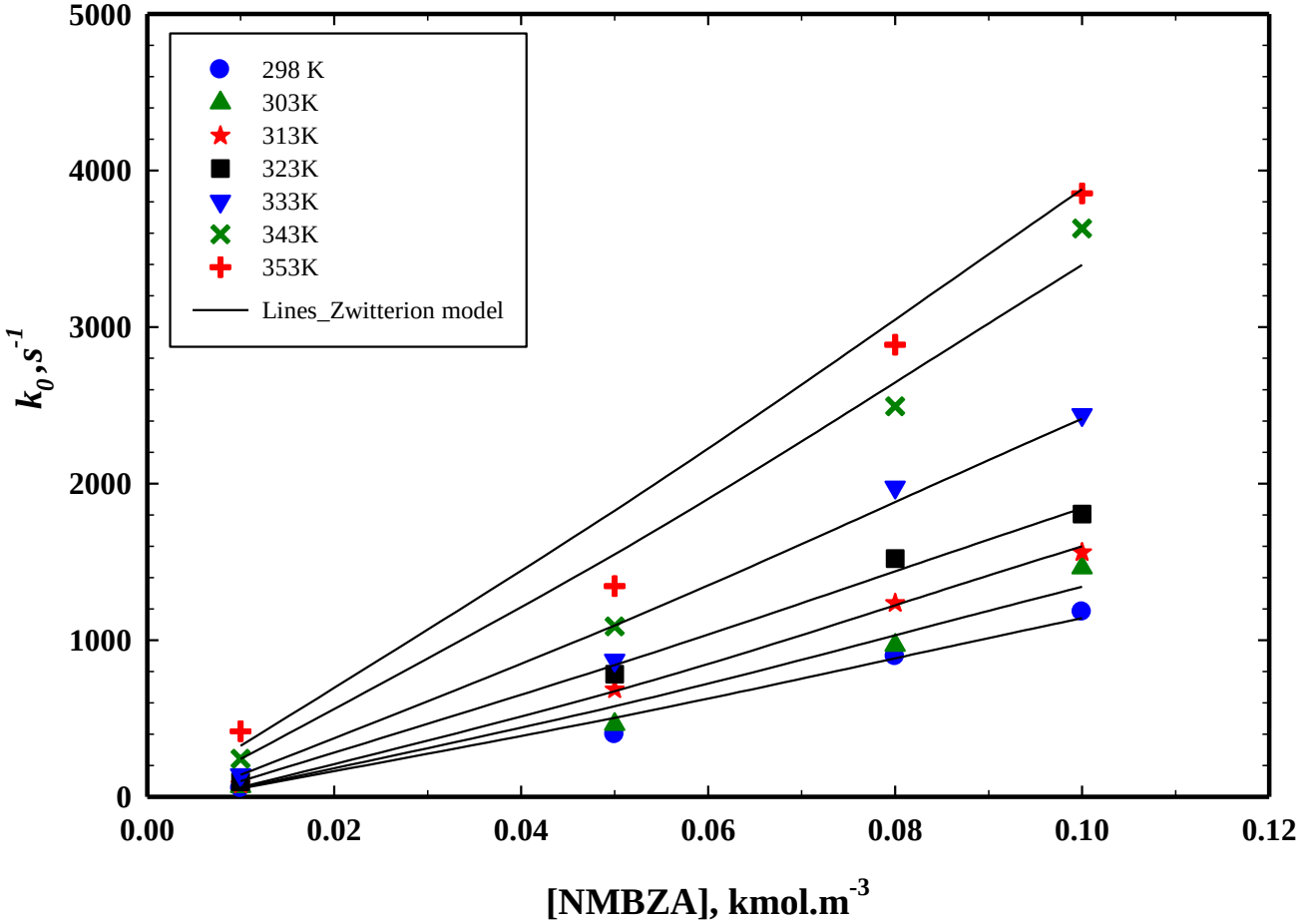

Figure 4. Measured reaction kinetics of aqueous NMBZA with CO_2 (hydrophilic system) using stopped-flow equipment at low concentrations compared to the zwitterion model

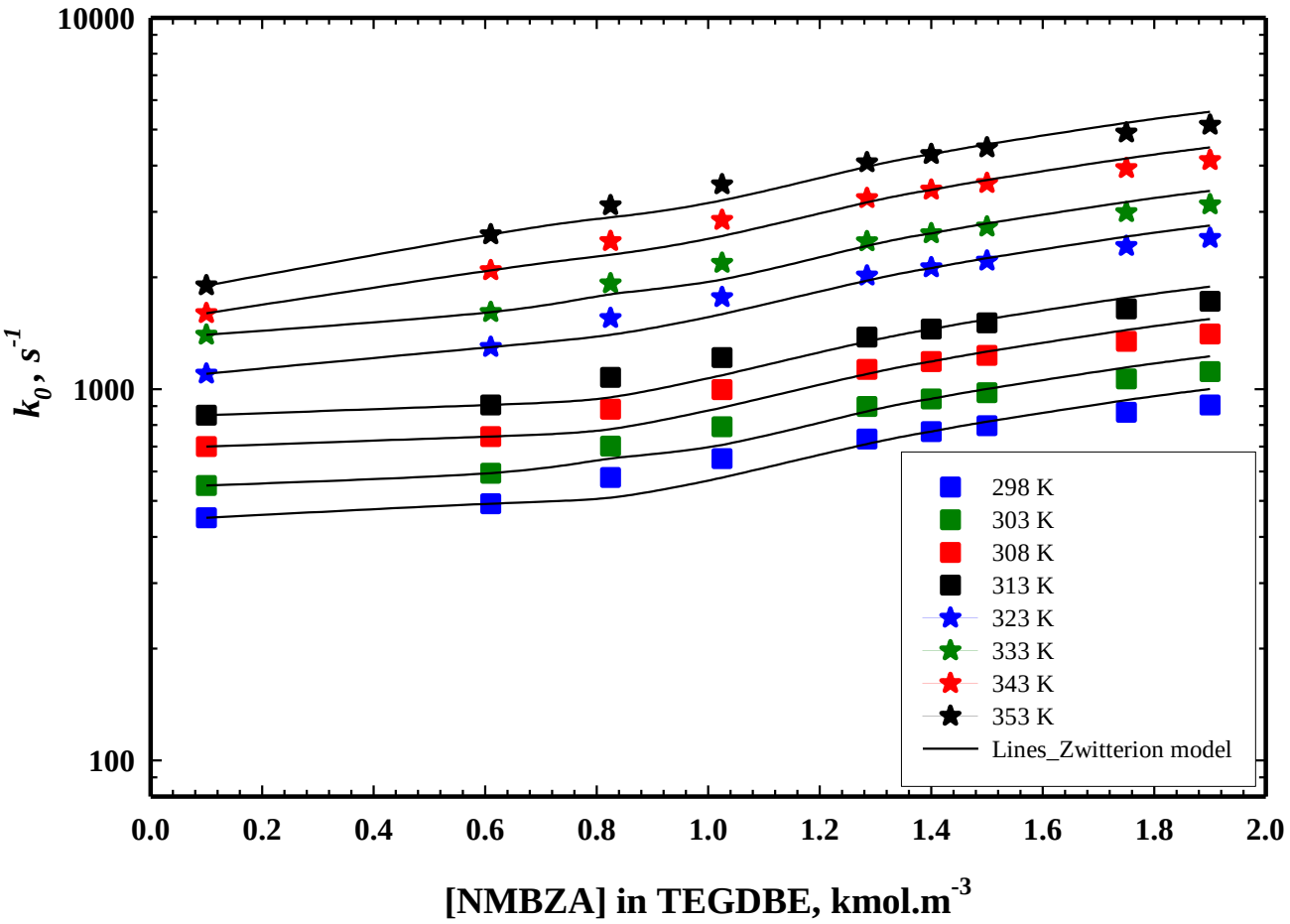

Figure 5. Measured reaction kinetics of NMBZA + H_2O + TEGDBE with CO_2 (hydrophobic system) using stopped-flow apparatus at low concentrations compared to the zwitterion model

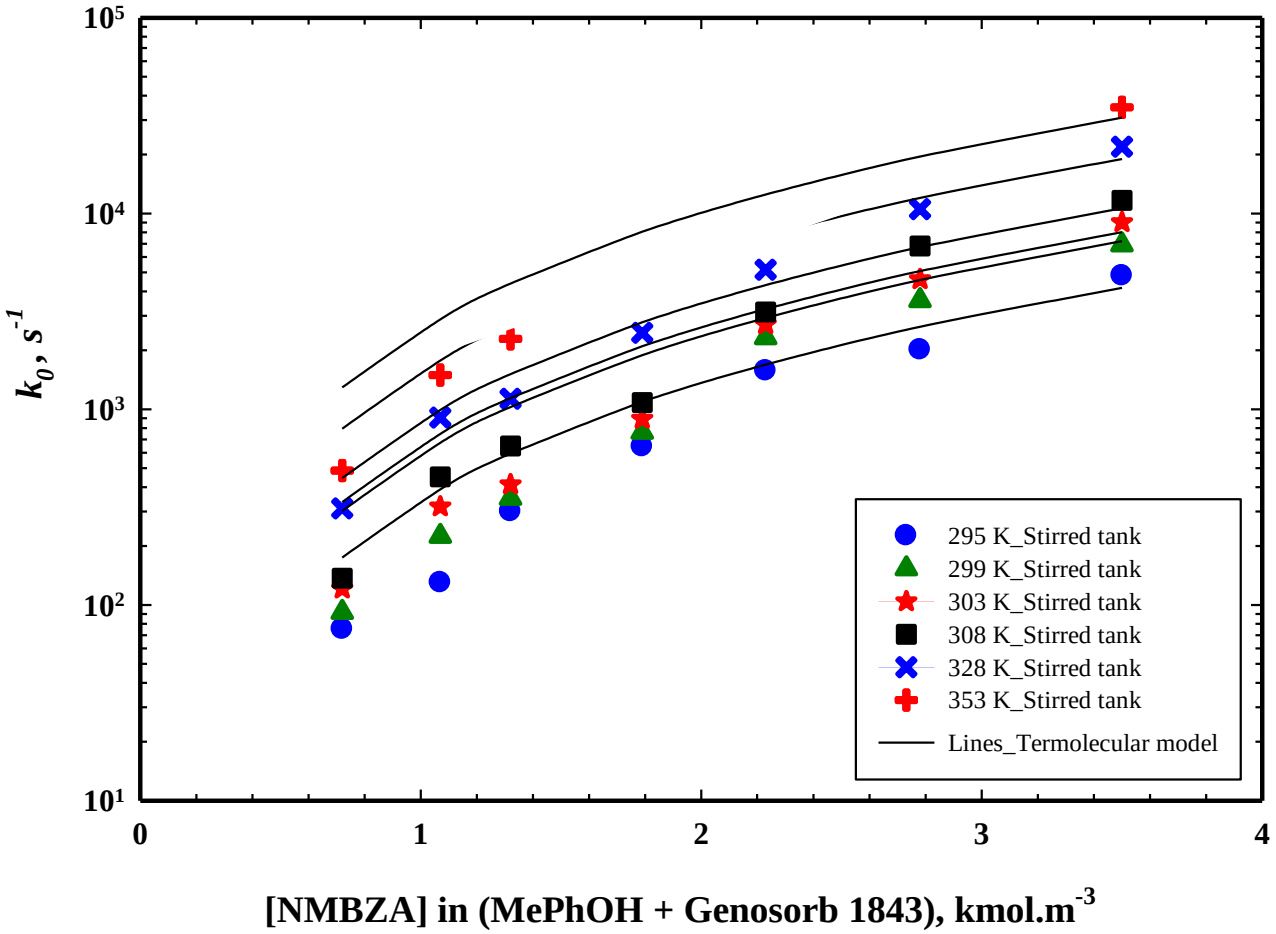

Figure 6. Measured reaction kinetics of NMBZA + MePhOH + Genosorb 1843 with CO_2 (hydrophobic system) using Stirred-tank reactor at high concentrations compared with the termolecular mode

Table 3. Calculated values of the empirical equation (Equation 9) for calculating the pseudo-first order rate constants (k_0) at different temperatures and concentrations

	k_0 = m *[Amine]^n =					
System	***A***	***B***	***C***	***D***	***E***	***R²***
MEA + H_2O	1.23	5.92E-02	2.00E-04	-1.88E-02	1.36	0.99
NMBZA + H_2O	0.54	5.00E-02	1.60E-03	2.00E-02	1.04	0.99
NMBZA + H2O + TEGDBE	8.92	2.32E-02	-2.00E-05	3.70E-03	0.46	0.99
NMBZA + MePhOH + Genosorb 1843	3.00E-07	4.99E-02	0.00E+00	-2.50E-03	2.84	0.98

Table 4. Calculated second-order reaction rate constants for aqueous MEA using different mechanisms

		k_2 ($m^3.mol^{-1}.s^{-1}$)						
Mechanism	**Equation**	**298.15**	**303.15**	**313.15**	**323.15**	**333.15**	**343.15**	**353.15**
Zwitterion	Equation 1	5.9	7.7	8.6	11.3	14.1	18.0	29.9
Zwitterion	Equation 2	5.0	6.0	8.5	10.8	13.8	17.1	27.8
Termolecular	Equation 3	4.6	5.7	8.1	10.7	13.2	16.6	26.2
Zwitterion or Termolecular	Equation 4	5.0	5.5	6.5	7.3	8.3	9.2	11.7

Table 5. Calculated second-order reaction rate constants for aqueous NMBZA using different mechanisms

		k_2 ($m^3.mol^{-1}.s^{-1}$)						
Mechanism	**Equation**	**298.15**	**303.15**	**313.15**	**323.15**	**333.15**	**343.15**	**353.15**
Zwitterion	Equation 1	13.1	16.0	19.7	20.4	27.1	39.2	43.9
Zwitterion	Equation 2	11.1	13.1	15.3	18.0	23.6	33.2	36.2
Termolecular	Equation 3	10.3	12.1	14.5	17.1	22.2	31.5	34.8
Zwitterion or Termolecular	Equation 4	4.8	5.2	5.6	6.1	7.0	8.3	8.6

Table 6. Calculated second-order reaction rate constants for NMBZA + CO_2 in TEGDBE (hydrophobic) using different mechanisms

		k_2 ($m^3.mol^{-1}.s^{-1}$)							
Mechanism	**Equation**	**298.15**	**303.15**	**308.15**	**313.15**	**323.15**	**333.15**	**343.15**	**353.15**
Zwitterion	Equation 1	0.55	0.67	0.85	1.04	1.52	1.88	2.46	3.07
Zwitterion	Equation 2	0.54	0.66	0.83	1.02	1.50	1.84	2.64	3.01
Termolecular	Equation 3	0.53	0.67	0.84	1.04	1.50	1.88	2.46	3.17
Zwitterion or Termolecular	Equation 4	0.56	0.68	0.86	1.09	1.59	1.96	2.58	3.21

Table 7. Calculated second-order reaction rate constants for NMBZA +MePhOH + Genosorb 1843 in TEGDBE (hydrophobic) using different mechanism

		k_2 ($m^3.mol^{-1}.s^{-1}$)					
Mechanism	**Equation**	**295.15**	**299.15**	**303.15**	**308.15**	**328.15**	**353.15**
Zwitterion	Equation 1	1.74	1.15	0.90	0.68	0.38	0.22
Zwitterion	Equation 2	0.88	1.52	1.68	2.26	4.01	6.59
Termolecular	Equation 3	0.64	1.13	1.25	1.62	2.97	4.88
Zwitterion or Termolecular	Equation 4	0.65	1.13	1.25	1.66	2.97	4.82

Table 8. Best fit mechanisms with their expression to determine the pseudo-first order rate constants (k_0) and second order reaction rate constants (k_2)

Studied System	**Mechanism-Best fit**	**AAD%**	**Kinetic expression**
(MEA + H_2O)	Termolecular mechanism	5	
(NMBZA + H_2O)	Zwitterionic mechanism	10	
(NMBZA + H_2O + TEGDBE)	Termolecular mechanism	8	
(NMBZA + MePhOH + Genosorb 1843)	Termolecular mechanism	25	

4.2. Experimental Discussion

4.2.1. Hydrophilic systems

4.2.1.1. MEA + H_2O system

A detailed literature survey was made over the timespan of 1961-2017 for the study regarding reaction kinetics of aqueous MEA with CO_2 and listed in Supplemental Information (Table 16). It was found that all of the experiments were conducted in the temperature range of 295-333 K except Leder [31] who reported a second order reaction rate constant (k_2) at 353 K using a stirred vessel. But it was found that the value reported lies away from the trend of other reported literature values, including this work, as shown in Figure 7. It was found that equation 14, which corresponds to the termolecular mechanism ($k_2^T = k_{MEA}[MEA] + k_{H2O}[H_2O]$), correlated the data in this work well. This shows that the intermediate loosely bound complex, which may be zwitterion, is deprotonated by both MEA and water. From Figure 7, it can be seen that k_2 values from this work (blue circles) follow the Arrhenius trend for higher temperatures. The value reported by Leder [31] was found to be overestimated. Using the model developed in this work, the reaction rate of aqueous MEA with higher concentrations and higher temperatures were predicted and found to agree with the values reported by Aboudheir et al. [32] within 10 AAD% and given in Supplementary Information (Figure 18). It also gives confidence in extrapolating the reaction rate data using a well fit reaction mechanism at lower concentrations (stopped-flow data) to the higher concentration reaction rate that are usually obtained with a stirred-tank reactor, laminar jet apparatus, etc. as concluded by Kierzkowska-Pawlak et al.[25].

The activation energy calculated in this work for the solvent (k_2^T), MEA (k_{MEA}), and water (k_{H_2O}) are 25.71 kJ.mol^{-1}, 38.33 kJ.mol^{-1} and 24.99 kJ.mol^{-1} which are close to the values of k_{MEA} (36.68 kJ.mol^{-1}) and k_{H2O} (27.33 kJ.mol^{-1}) reported by Aboudheir et al. [32]. It is noted

that most of the literature listed in Supplemental Information (Table 16) reported a value of 44.9 kJ.mol^{-1} [28].

4.2.1.2. NMBZA +H_2O system

Activation energies calculated in this work for the solvent (k_2^Z), NMBZA (k_{NMBZA}) and water (k_{H_2O}) are 18.77 kJ.mol^{-1}, 27.66 kJ.mol^{-1} and 203.48 kJ.mol^{-1}. Temperature dependency of water on the reaction rate is negligible compare to NMBZA, that may be the reason for higher activation energy for water in this system compare to aqueous MEA system. Using the model developed in this work, the reaction rate of aqueous NMBZA with high concentrations and temperatures were predicted and given in Supplemental Information (Figure 19). These values can be used in process modeling to design the absorber column required for CO_2 capture using aqueous NMBZA. The reaction rate of CO_2 with aqueous NMBZA from this study at 313 K was compared with other promising solvents used for CO_2 capture processes as shown in Figure 8. It was found that aqueous NMBZA has a reaction rate higher than primary amines monoethanolamine (MEA) and benzyl amine (BZA; [19]), secondary amines ethyl ethanolamine (EEA; [33]) and 2-aminoethylethanolamine (AEEA; [6]), but lower than aromatic secondary amine piperazine (Pz; [34]). Because of the aromatic functionality which stabilizes the availability of the lone pair of electrons in the amino group, NMBZA may have a higher reaction rate than other amines in Figure 8, which is a similar trend reported in the literature [34].

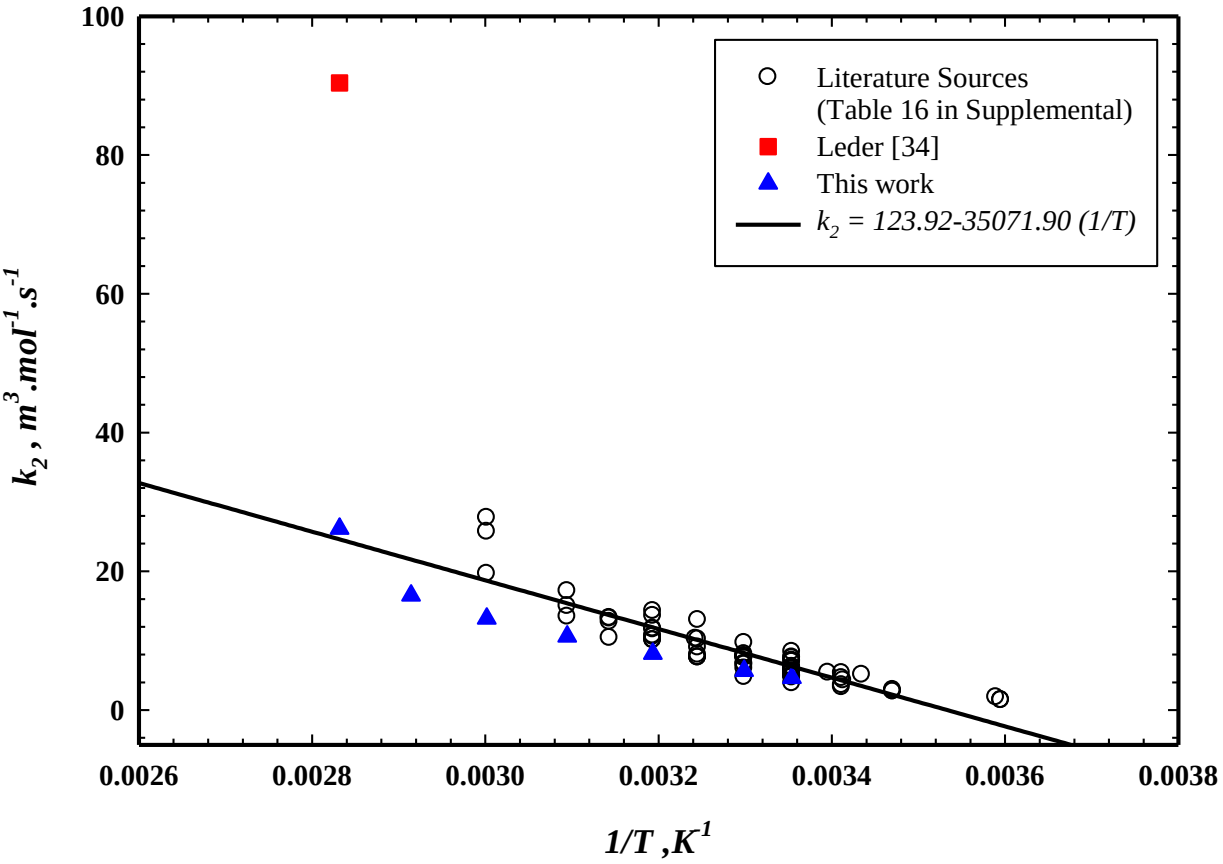

Figure 7. Comparison of Arrhenius plots to predict second order reaction rate constants (k_2) at different temperatures for MEA + H_2O + CO_2 (hydrophilic) system

4.2.2. Hydrophobic system

4.2.2.1. (NMBZA + H_2O + TEGDBE) and (NMBZA + MePhOH + Genosorb 1843)

Activation energies calculated in this work for the solvent (k_2^T), NMBZA ($k_{2,NMBZA}$) and TEGDBE (k_{TEGDBE}) are 27.98 kJ.mol^{-1}, 10.37 kJ.mol^{-1}, and 18.04 kJ.mol^{-1}, respectively. Using the model developed in this work, the reaction rate of CO_2 in a NMBZA + TEGDBE mixture with higher NMBZA concentrations and higher temperatures were predicted and given in Supplemental Information (Figure 20). Activation energies calculated in this work for the solvent (k_2^T) *and* NMBZA ($k_{2,NMBZA}, k_{NMBZA}$) are 27.19 kJ.mol^{-1}, 13.6 kJ.mol^{-1}, and 13.6 kJ.mol^{-1},

respectively. Using the model developed in this work, the reaction rate of CO_2 in (NMBZA + MePhOH + Genosorb 1843) mixture with lower and higher NMBZA concentrations and higher temperatures were predicted and given in Supplemental Information (Figure 21). These models could be used in a process model to design an absorber required for CO_2 capture using a non-aqueous solvent system containing NMBZA.

The reaction rate of CO_2 with non-aqueous NMBZA from this study at 313 K was compared with other promising non-aqueous solvents used for CO_2 capture processes as shown in Figure 9. It was found that the non-aqueous mixture of NMBZA + TEGDBE has similar reaction rate to that of diethanolamine (DEA) in polyethylene glycol (DEA + PEG400 [35]) at higher concentrations, but non-aqueous (NMBZA + MePhOH + Genosorb 1843) has a higher reaction rate than (DEA +PEG400 [35]) at higher concentrations. The reaction rate of CO_2 in non-aqueous ethylene diamine (EDA [36]) with methanol had the higher reaction rate among the chosen systems and the reaction rate of CO_2 with the mixture of a sterically hindered amine, 2-amino-2-methyl-1,3-propanediol (AMPD [37]) and methanol was found to be the lowest.

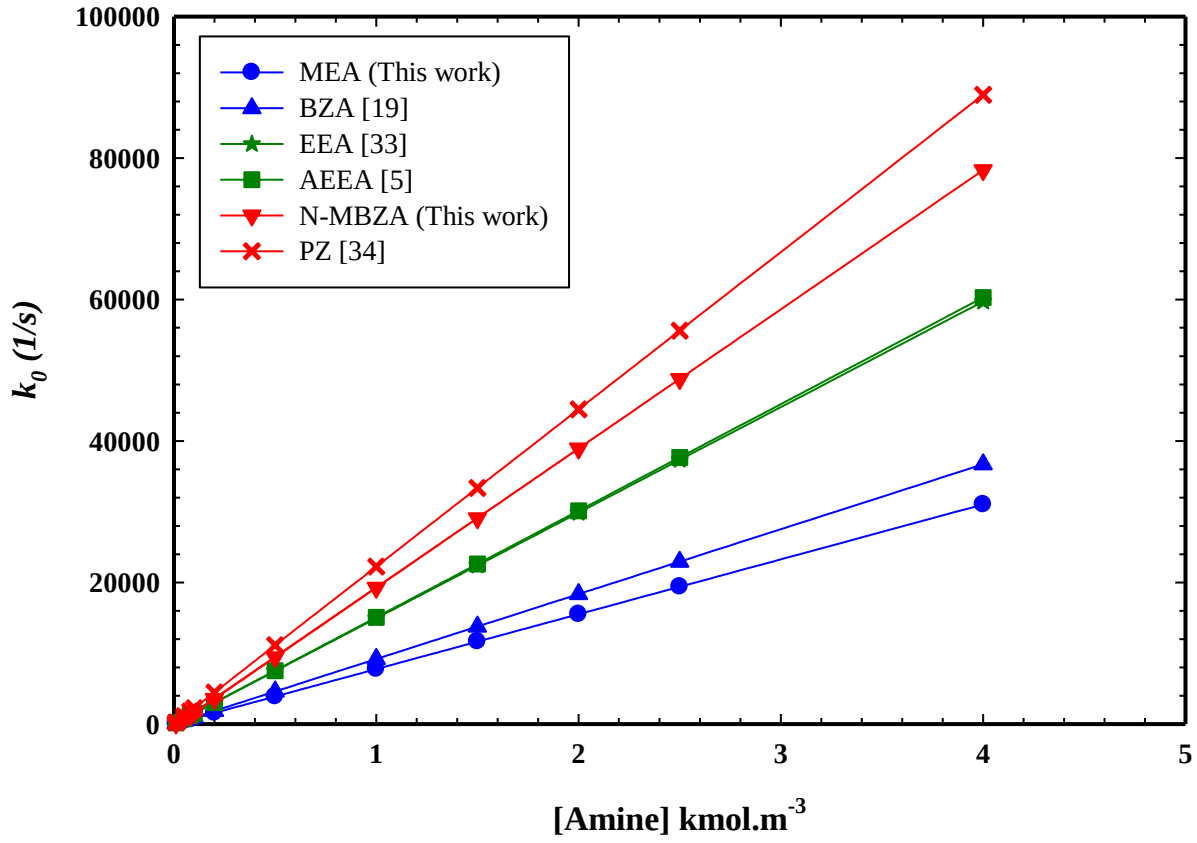

Figure 8. Comparison of reaction kinetics of different hydrophilic and hydrophobic amines at 313 K (Primary-Blue; Secondary-Green; Aromatic-Red)

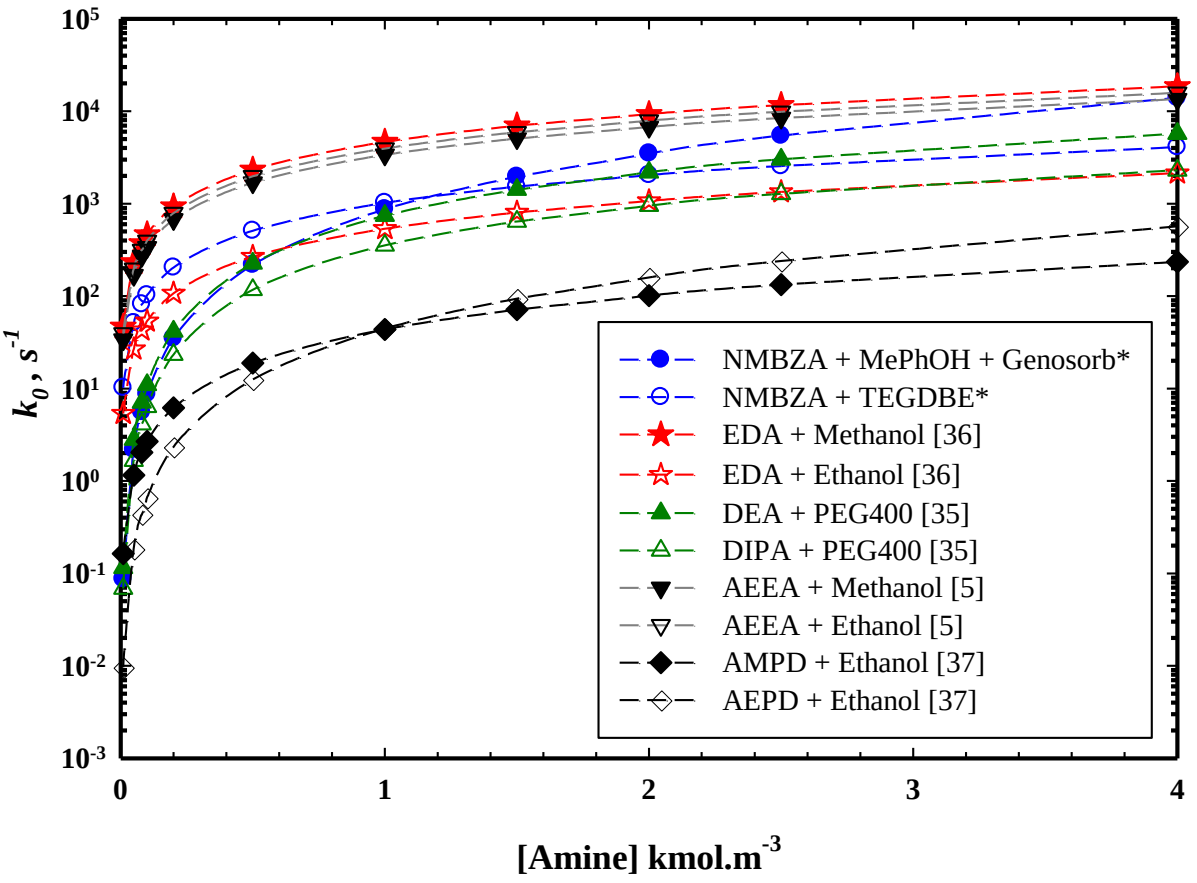

*Figure 9. Comparison of reaction kinetics of CO_2 with amines at 313 K (hydrophilic and hydrophobic) with different non-aqueous systems (Sterically hindered hydrophobic secondary amine-Blue; Primary amine-Red; Secondary amine-Green; Sterically hindered hydrophilic amines-Black);*This work*

4.2.2.2. (NMBZA + TEGDBE + activators (water, PZ, HPIP))

In order to find the effect of the addition of water and activators such as piperazine (Pz; Sparingly soluble in NMBZA + TEGDBE + H_2O) and 4-hydroxypiperidinol (HPIP; Completely

soluble in NMBZA + TEGDBE + H_2O) on the reaction rate of CO_2 with the NMBZA + TEGDBE mixture, stopped-flow experiments were conducted with an amine concentration in the range of 1.22-3.5 kmol.m^{-3}, water concentration in the range 0.52-3.97 kmol.m^{-3}, and activators in the concentration range of 0.45-0.93 kmol.m^{-3} (i.e., ~5-10 wt.%) at temperature ranges of 298-353 K. The obtained experimental values at different temperatures are given in Table 17. It was found that the reaction rate in reference to a base concentration (i.e., 1.75 kmol.m^{-3} NMBZA + 1.3 Water + 1.74 kmol.m^{-3} TEGDBE) increased with an increase in the concentration of water, Pz, and HPIP as shown in Table 17. This may be due to the deprotonation of the loosely bounded complex from the termolecular mechanism by the promoters such as water, Pz, and HPIP beside the dominating component in the solvent as suggested in the previous section. The reaction rate of CO_2 with the mixture increased 1.6 and 1.4 times when Pz and HPIP, respectively, increased from 0 to 1.09 kmol.m^{-3} and water increased from 2.61 to 3.97 kmol.m^{-3}. But Pz was found to be sparingly soluble compared to HPIP, which is completely soluble in the mixture. So, for this mixture, HPIP will be a better activator than Pz. An Arrhenius type equation was used to obtain the k_0 values at different temperatures as described below:

Equation 22:ln —

Where, *[NMBZA]*; *[NMBZA]* is in mol.m^{-3}; E_a is the activation energy in kJ.mol^{-1}; R is the gas constant – 8.314 J.mol^{-1}.K^{-1}; and T is the temperature in K. Fitted constants are given in Table 9 with their R^2 values. The fitted k_2 values and comparison of the effect of adding water, amine, Pz, and HPIP with respect to temperature are given in Supplemental Information (Figure 22, Figure 23, and Figure 24). Increases in reaction rate with the addition of activators are more predominant at higher temperatures than at lower temperatures as shown in Figure 10. Activation energies of Pz and HPIP with respect to temperature are found to be similar with

values 32.83 kJ.mol^{-1} and 33.51 kJ.mol^{-1}, respectively. Activation energy of adding amine to the reference mixture was found to increase from 22.22 to 26.78 kJ.mol^{-1}. The activation energy of adding Pz to the reference mixture was found to increase from 21.34 to 26.85 kJ.mol^{-1}. The activation energy of adding Pz and water to the mixture was found to increase from 21.34 to 32.83 kJ.mol^{-1}. The activation energy of adding HPIP and water to the mixture was found to increase from 21.34 to 33.51 kJ.mol^{-1}. Equation 22 could be used in a process model to design an absorber required for CO_2 capture using (NMBZA + TEGDBE) mixture with water and activators Pz or HPIP.

Table 9. Calculated Arrhenius constants (Eq.36) required to calculate second-order reaction rate constants (k_2-$m^3.mol^{-1}.s^{-1}$) for the studied system

Concentration ($kmol.m^{-3}$)	**Effect of concentration of water**			**Effect of concentration of Pz**			**Effect of concentration of water and Pz**		**Effect of concentration of water and HPIP**	
[NMBZA]	**0.61**	**0.61**	**1.75**	**1.75**	**1.75**	**1.75**	**1.75**	**1.75**	**1.75**	**1.75**
***[PZ]* or [HPIP]**	**0.00**	**0.00**	**0.00**	***0.05***	***0.22***	***0.44***	***0.44***	***0.55***	**0.23**	**0.46**
[water]	**0.26**	**1.30**	**1.30**	**1.30**	**1.30**	**1.30**	**1.98**	**1.98**	**1.98**	**1.98**
[TEGDME]	**1.45**	**1.38**	**0.87**	**0.85**	**0.80**	**0.73**	**0.68**	**0.65**	**0.74**	**0.65**
E_a ($kJ.mol^{-1}$)	21.34	22.22	26.78	26.71	26.99	26.85	28.37	32.83	28.24	33.51
A ($m^3.mol^{-1}.s^{-1}$)	4.02E+09	6.29E+09	5.81E+10	5.89E+10	7.07E+10	7.04E+10	1.29E+11	8.66E+11	1.22E+11	9.68E+11
R^2	0.92	0.94	0.99	0.99	0.99	0.99	0.99	0.99	0.94	0.97

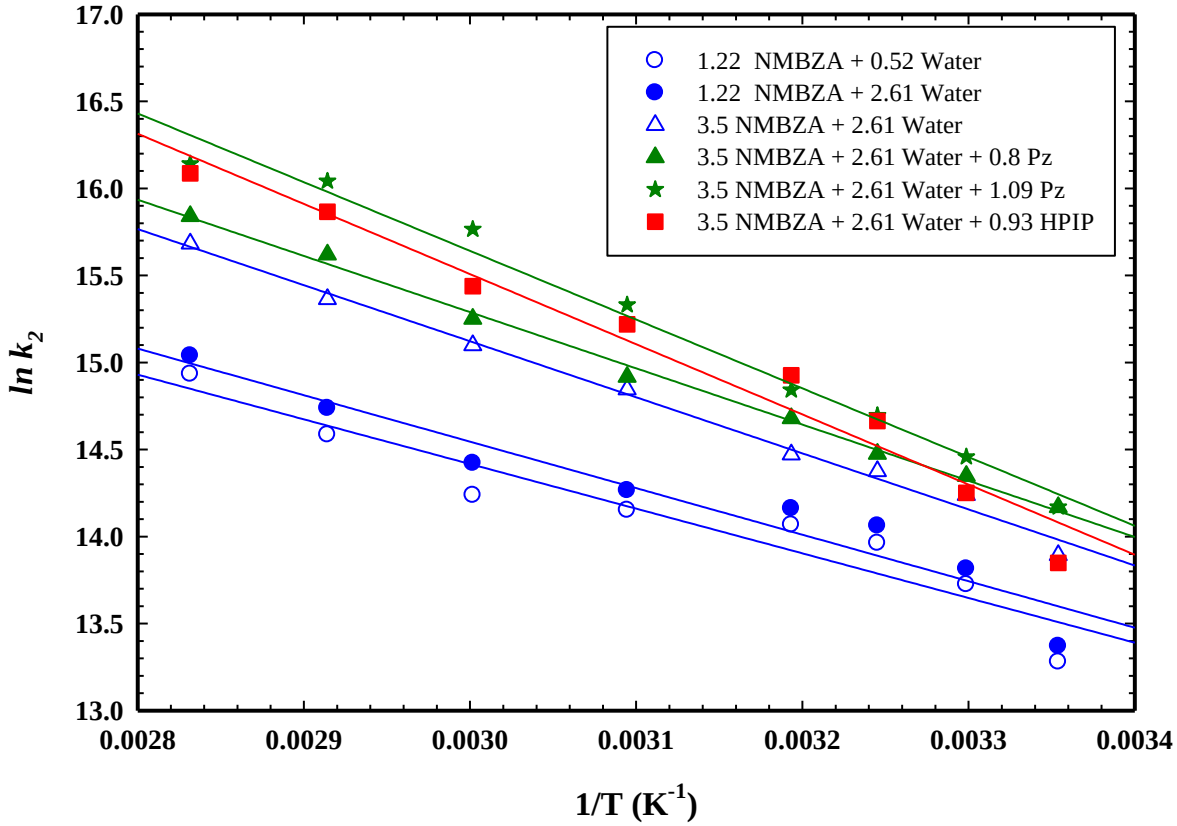

Figure 10. Comparison of second-order reaction rate constants of CO_2 with mixture of NMBZA + TEGDBE (hydrophobic system) with different concentration of water and with the addition of different activators (Pz and HPIP) at different temperatures. Lines are Arrhenius equation fits using Equation 22.

4.2.3. Comparison of system studied in this work

All the systems in this study were compared with each other at 313 K in Figure 11. It was found that aqueous NMBZA has the highest reaction rate with CO_2 compared to non-aqueous solvents, followed by aqueous MEA. The non-aqueous hydrophobic solvents NMBZA + TEGDBE with the addition of HPIP and water has the highest reaction rate followed by the addition of Pz and water. NMBZA with TEGDBE without any deprotonating additives has the lowest reaction rate. This result indicates that the CO_2 amine reaction rate of non-aqueous solvent can be tailored with the presence of deprotonating additives. Among the additives examined in this study, HPIP was found to be similar to Pz but better in terms of solubility in the solvents and MePhOH + Genosorb 1843. The activation energies of these system, shown in Table 10, also support this conclusion. It can be observed that the activation energy for NMBZA is lower in TEGDBE and increases as additives are added to the system. Activation energies of solvents follow the order of: TEGDBE + H_2O = MePhOH + Genosorb 1843 < TEGDBE + Pz + H_2O < TEGDBE + HPIP + H_2O. The activation energy for the CO_2 reaction of the solvent is reduced from aqueous to non-aqueous systems. However, it increased by adding the deprotonating agents such as MePhOH, Pz, and HPIP.

5. Conclusions

In this work, the reaction kinetics of absorption of CO_2 with N-methyl benzyl amine (NMBZA) in aqueous and non-aqueous solutions (Tetra ethylene dibutyl ether (TEGDBE); mixture of 4-methoxy Phenol (MePhOH) and polyethylene glycol dibutyl ether (Genosorb 1843)) were studied using a stopped-flow apparatus and a stirred tank reactor in a concentration range of 0.01-4 $kmol.m^{-3}$ along with aqueous solutions of monoethanolamine (MEA) at a temperature range of 295-353 K. The reaction orders were found to be 0.9, 1.2, 0.6 and 2.7 for

(MEA + H_2O), (NMBZA + H_2O), (NMBZA + TEGDBE), and (NMBZA + MePhOH + Genosorb 1843), respectively. Three solvents were used in the analysis of the reaction kinetics of CO_2 with NMBZA in aqueous hydrophilic and hydrophobic solvents (H_2O, TEDBE, MePhOH + Genosorb 1843). The reaction rate follows the order of: H_2O < MePhOH + Genosorb 1843 < TEGDBE. Three activators were added to promote the reaction rate of CO_2 with NMBZA in TEGDBE (H_2O, piperazine (Pz), Hydroxy Piperidinol (HPIP). It was found that HPIP, which is completely soluble in the mixture, promotes the reaction rate with CO_2 similar to Pz, which is only slightly soluble. The zwitterion and termolecular mechanisms with dominating deprotonating components for the zwitterion or loosely bound complex were found to fit the reaction rate and could be used to interpret the reaction data. Deprotonation of the loosely bound complex increased with the addition of activators such as water, Pz, and HPIP to the solvent. Second-order reaction rate constants for these systems could be derived at different concentrations of NMBZA at different temperatures using the Arrhenius expression provided in this work, and could be used for designing an absorber column for CO_2 capture processes using aqueous and non-aqueous solvents. The mixture of NMBZA + TEGDBE and HPIP was shown to be the best solvent among the studied system for CO_2 capture processes using non-aqueous solvents.

Nomenclature

A Arrhenius constant ($m^3.mol^{-1}.s^{-1}$)

AAD absolute average deviation

B base (amine, water, ethanol, methanol or hydroxyl ion)

E_a activation energy ($kJ.mol^{-1}$)

k_0	observed pseudo-first-order reaction rate constant (s^{-1})
k_{-1}	backward first-order reaction rate constants (s^{-1})
	forward second-order reaction rate constant in zwitterion mechanism ($m^3.mol^{-1}.s^{-1}$)
	forward second-order reaction rate constant in termolecular mechanism ($m^3.mol^{-1}.s^{-1}$)
r_{CO2}	rate of reaction with respect to CO_2 ($mol.m^{-3}s^{-1}$)
R	universal gas constant (0.008315 $kJ.mol^{-1}.K^{-1}$)
T	temperature (K)
t	time (s)
Y	measure of the signal obtained (V)
	constant value of the signal (V) at equilibrium
[ ]	concentration ($kmol.m^{-3}$)

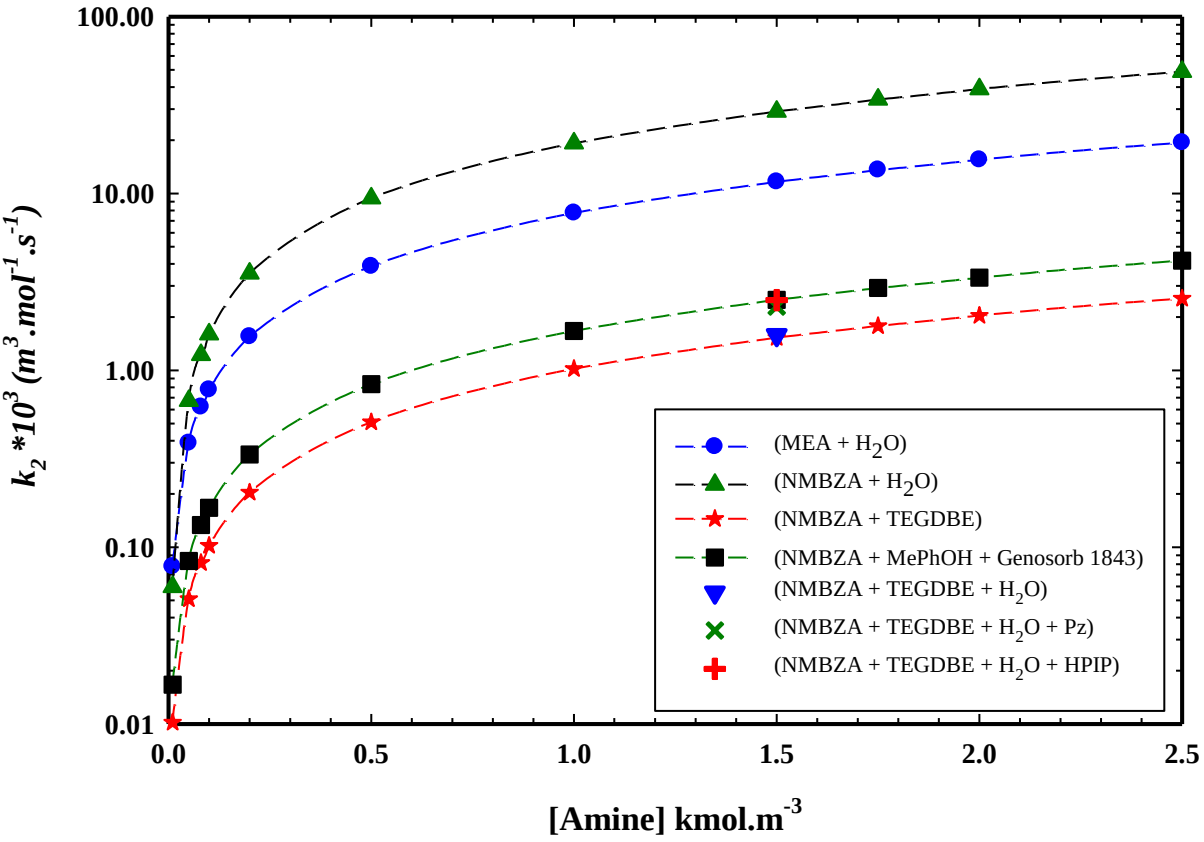

Figure 11. Calculated second-order reaction rates of studied solvents with CO_2 in this work

Table 10. Activation energies of the solvents with CO_2 studied in this work

System	Solvent	Solubility Parameter $(J.m^{-3})^{1/2}$	(Amine + Solvent) Type	Order	Mechanism	Activation Energy ($kJ.mol^{-1}$) E_{amine}	$E_{solvent}$
MEA	H_2O	47.9	Hydrophilic	0.9	Termolecular	36.68	27.33
N-MBZA	H_2O	47.9	Hydrophilic	1.2	Zwitterion	27.66	18.77
N-MBZA	TEGDBE	19.4	Hydrophobic	0.6	Zwitterion or Termolecular	10.37	27.98
N-MBZA	MePhOH + Genosorb 1843	20.5	Hydrophobic	2.6	Termolecular	13.60	27.19
N-MBZA	TEGDBE + H_2O	20.2	Hydrophobic	--	Arrhenius-Fit	--	26.78
N-MBZA	TEGDBE + Pz + H_2O	20.1	Hydrophobic	--	Arrhenius-Fit	--	32.83
N-MBZA	TEGDBE + HPIP + H_2O	20.1	Hydrophobic	--	Arrhenius-Fit	--	33.51

Acknowledgements

RTI would like to acknowledge the United States Department of Energy/National Energy Laboratory (DOE/NETL) for funding the development of this technology under co-operative agreements DE-FE0013865 and DE-FE0026466, respectively. Additionally, RTI would like to acknowledge partnership with BASF Corp, BASF SE, Linde LLC, and SINTEF.

Supporting Information:

Table 11. Kinetic studies of amines in non-aqueous media (both hydrophobic and hydrophilic system)

Equipment	**Author**	**Year**	**T/K**	**System Studied**
Stirred-tank	Sada et al. [38-40]	1985	303	EDA in (methanol, ethanol, ethylene glycol)
		1986	303	MIPA in cyclohexylamine
		1989	303	MEA, DEA & TEA in (methanol, ethanol, 2-propanol)
	Versteeg et al. [41]	1988	298-313	DEA&DIPA in (ethanol and n-butanol)
	Henni	2002	288-313	MDEA in sulfone
	Park et al. [42, 43]	2006	298	TEA and MDEA in (methanol, ethanol, n-propanol, n-butanol, ethylene glycol, propylene glycol and propylene carbonate)
Stopped-flow	Ali et al. [44]	2000	278-293	Aniline, cyclohexane, hexamine in ethanol
	Crooks & Donnellan	1988	298	DEA in ethanol
	Li [45]	2006	293-313	AEEA in (methanol, ethanol)
	Kadiwala et al. [36]	2012	293-313	EDA, 3-AP in (methanol, ethanol)
	Rayer at al. [6]	2013	293-313	AEEA in (methanol, ethanol)
	Duatepe and Alper [37]	2017	288-308	AMPD, AEPD in ethanol
	Ozturk et al. [9]	2014	288-308	1,1,3,3-tetramethylguanidine (TMG) in 1-hexanol
	Ozturk et al. [46]	2012	288-308	1,8-Diazabicyclo[5.4.0]undec-7-ene (DBU) in alkanol
	Ozturk [9]	2014	288-308	CO_2 BOL in alkanols

	Orhan, O. Y [12]	2014	288-308	CO_2 into Ionic Liquid-CO2 BOL hybrid system
	Orhan, O. Y et al.	2017	288-308	CO_2 BOL in hexanol
	Zhong et al.	2016	293-313	TERA in methanol and ethanol
Wetted sphere	Davis and Sandall [35]	1993	293-313	DEA, DIPA in (polyethylene glycol)
	Mathias et al. [47]	2015	308-328	MEA, PZ, First-Generation CO_2 BOL, Second-generation CO_2 BOL
	Whyatt et al. [48]	2016	308-328	MEA and First-Generation CO_2 BOL
	Heldebrant et al. [49]	2005	308-328	1,8-Diazabicyclo[5.4.0]undec-7-ene (DBU) in alkanol

Table 12. Experimental kinetic data for MEA + CO_2 in water (hydrophilic) from stopped-flow apparatus

Concentration		**Pseudo first-order rate constant (k_0)**						
(mol.m^{-3})		***T (K)***						
[Water]	**[MEA]**	**298**	**303**	**313**	**323**	**333**	**343**	**353**
55460	10	49	70	112	154	190	255	328
55324	50	227	282	405	534	658	823	1302
55223	80	373	455	644	820	1040	1288	2097
55155	100	525	636	894	1118	1439	1773	2929
Reaction Order (*n*)		1.00	0.93	0.87	0.83	0.85	0.81	0.92

Table 13. Experimental kinetic data for NMBZA + CO_2 in water (hydrophobic) from stopped-flow apparatus

Concentration (mol.m^{-3})		**Pseudo first-order rate constant (k_0)**						
		T (K)						
[Water]	**[NMBZA]**	**298**	**303**	**313**	**323**	**333**	**343**	**353**
56093	10	52	65	78	94	139	242	417
55824	50	504	587	724	855	1092	1543	1704
55622	80	885	1044	1223	1442	1885	2653	2894
55487	100	1140	1348	1555	1834	2413	3392	3688
Reaction Order (n)		1.36	1.32	1.31	1.3	1.25	1.14	0.94

Table 14. Experimental kinetic data for NMBZA +H_2O + CO_2 in TEGDBE (hydrophobic) from stopped-flow apparatus

Concentration (mol.m^{-3})			**Pseudo first-order rate constant (k_0)**							
			T (K)							
[Water]	**[Solvent]**	**[NMBZA]**	**298**	**303**	**308**	**313**	**323**	**333**	**343**	**353**
2776	5911	25	407	512	633	824	915	1073	1278	1453
2776*	5821*	100*	450*	550*	700*	850*	1100*	1400*	1600*	1900*
2776	5761	610	491	594	745	906	1297	1611	2087	2606
2776	5694	825	578	702	882	1075	1552	1924	2502	3123
2776	5625	1025	650	792	996	1215	1766	2186	2851	3558
2776	5528	1285	734	897	1131	1381	2020	2496	3266	4074
2776	5481	1400	768	941	1186	1450	2126	2626	3438	4289
2776	5440	1500	797	978	1233	1507	2215	2734	3584	4470
2776	5329	1750	866	1065	1344	1645	2427	2994	3931	4902
2776	5258	1900	906	1115	1408	1723	2549	3142	4131	5150
Reaction Order (n)			0.54	0.55	0.56	0.57	0.59	0.59	0.6	0.6

* Extrapolated data for comparison with aqueous data

Table 15. Experimental kinetic data for NMBZA + MePhOH + CO2 in Genosorb 1843 (hydrophobic) from stirred-tank reactor

Concentration (mol.m-3)			Pseudo first-order rate constant (k0) T (K)					
[Water]	[Solvent]	[NMBZA]	295	299	303	308	328	353
4219	6878	716	75	92	121	137	311	486
4219	6701	1069	130	225	318	451	906	1493
4219	6565	1319	300	352	412	648	1130	2285
4219	6285	1790	643	763	892	1080	2459	6128
4219	5996	2227	1569	2323	2711	3141	5160	8565
4219	5589	2784	2010	3594	4601	6812	10521	17190
4219	5001	3499	4806	6932	9001	11661	21935	34852
Reaction Order (n)			2.7	2.82	2.78	2.81	2.65	2.65

Table 16. Kinetic studies of CO_2 with aqueous MEA +H_2O (hydrophilic system)

Equipment	**Author**	**Year**	**T/K**	k_2
Laminar Jet	Astarita [50]	1961	295	5.40
Wetted wall	Emmert and Pigord [51]	1962	298	5.40
Laminar Jet	Clarke [52]	1964	298	7.50
Laminar Jet	Sharma [53]	1965	298-303	
Laminar Jet	Danckwerts and Sharma	1966	291-308	5.1-13
Stirred-tank	Leder [31]	1971	353	90.40
Laminar Jet	Sada et al. [55-57]	1976	298	7.14-8.4
Rapid mixing	Hikita et al. [58, 59]	1977-1979	279-308	1.84-10.28
Wetted wall	Alvarez-Fuster et al. [60]	1980	293	4.30
Membranes	Donaldson and Nguyen [61]	1980	298	6.00
Stirred-tank	Laddha and Danckwerts	1981	298	5.87
Stopped flow	Penny and Ritter [63]	1983	278-303	1.45-6.53
Stirred-tank	Sada et al. [38]	1985	303	7.74
Stopped flow	Barth et al. [64]	1986	293-298	3.6-4.7
Stopped flow	Crooks and Donnellan [24]	1989	298	3.88
Stopped flow	Alper [65]	1990	278-298	1.44-5.6
Stirred-tank	Littel et al. [66]	1992	318-333	10.4-25.7
Laminar Jet	Hagewiesche et al. [67]	1995	313	10.09
Literature data	Versteeg et al. [41]	1996	298-313	5.99-14.27
Wetted wall	Xiao et al. [68]	2000	303-313	4.77-11.74
Wetted wall	Horng and Li [69]	2002	303-313	5.99-10.55
Laminar Jet	Abudheir et al. [32]	2003	303-333	5.34-19.64
Stopped flow	Ali [28]	2005	298-313	5.52-13.6
Laminar Jet	Edali et al. [70]	2009	298-323	6.24-14.99
Stopped flow	Conway et al. [71]	2011	288-318	2.7-13.2
Stopped flow	Richner et al. [19]	2015	288-318	2.7-13.8

Table 17. Experimental kinetic data for NMBZA + TEGDBE (hydrophobic) with different water, Pz, and HPIP concentrations at different temperatures from Stopped-flow apparatus

Concentration ($kmol.m^{-3}$)	**Effect of concentration of water**			**Effect of concentration of Pz**			**Effect of concentration of water and Pz**		**Effect of concentration of water and HPIP**	
[NMBZA]	**1.22**	**1.22**	**3.50**	**3.50**	**3.50**	**3.50**	**3.50**	**3.50**	**3.49**	**3.49**
Activators	**0.00**	**0.00**	**0.00**	***0.11***	***0.45***	***0.87***	***0.87***	***1.09***	**0.46**	**0.93**
[water]	**0.52**	**2.61**	**2.61**	**2.61**	**2.61**	**2.61**	**3.97**	**3.97**	**3.97**	**3.97**
[TEGDME]	**2.90**	**2.76**	**1.74**	**1.70**	**1.59**	**1.46**	**1.37**	**1.30**	**1.48**	**1.30**
T (K)	**Pseudo first-order rate constant (k_0)**									
298.15	481	526	888	941	1028	1169	1170	1170	828	849
303.15	749	820	1253	1316	1356	1398	1410	1560	1406	1269
308.15	951	1050	1438	1500	1575	1587	1657	1980	1891	1917
313.15	1056	1160	1582	1605	1819	1947	1879	2292	2335	2493
323.15	1149	1287	2300	2358	2500	2471	2544	3736	3101	3342
333.15	1252	1504	2964	3185	3387	3448	3558	5769	3573	4162
343.15	1772	2062	3861	3902	4473	4987	5421	7604	4989	6383
353.15	2510	2788	5312	5623	5923	6223	6884	8404	5964	7955

Table 18. Physicochemical data for (CO_2 + NMBZA + MePhOH + Genosorb 1843) system required to calculate mass transfer coefficients in a stirred tank reactor

Concentration (kmol.m^{-3})			**Density (kg.m^{-3})**			
[NMBZA]	**[MePhOH]**	**Genosorb-1843**	**295.15**	**308.15**	**328.15**	**353.15**
0.72	0.78	3.07	988.77	977.42	960.03	938.15
1.07	1.20	2.72	994.78	983.38	966.02	944.17
1.32	1.48	2.47	998.89	987.46	970.12	948.30
1.79	1.98	2.03	1006.19	994.71	977.41	955.64
2.23	2.48	1.61	1013.66	1002.13	984.88	963.15
2.78	3.11	1.07	1023.04	1011.44	994.24	972.58
3.50	3.88	0.39	1035.02	1023.34	1006.22	984.66
Concentration (kmol.m^{-3})			**Viscosity (cP)**			
[NMBZA]	**[MePhOH]**	**Genosorb-1843**	**295.15**	**308.15**	**328.15**	**353.15**
0.72	0.78	3.07	4.99	3.65	2.37	1.69
1.07	1.20	2.72	5.63	3.84	2.65	1.80
1.32	1.48	2.47	6.78	4.61	3.07	1.90

1.79	1.98	2.03	8.90	5.25	3.33	2.07
2.23	2.48	1.61	9.79	6.59	3.90	2.25
2.78	3.11	1.07	14.70	8.58	4.54	2.44
3.50	3.88	0.39	23.00	11.80	5.76	2.59

Concentration (kmol.m^{-3})			**Diffusivity of CO_2 (m.s^{-1})**			
[NMBZA]	**[MePhOH]**	**Genosorb-1843**	**295.15**	**308.15**	**328.15**	**353.15**
0.72	0.78	3.07	3.50E-10	5.00E-10	8.19E-10	1.24E-09
1.07	1.20	2.72	3.10E-10	4.75E-10	7.33E-10	1.16E-09
1.32	1.48	2.47	2.58E-10	3.96E-10	6.32E-10	1.10E-09
1.79	1.98	2.03	1.96E-10	3.47E-10	5.83E-10	1.01E-09
2.23	2.48	1.61	1.78E-10	2.77E-10	4.98E-10	9.29E-10
2.78	3.11	1.07	1.19E-10	2.13E-10	4.28E-10	8.57E-10
3.50	3.88	0.39	7.59E-11	1.55E-10	3.37E-10	8.07E-10

Concentration (kmol.m^{-3})			**Diffusivity of NMBZA (m.s^{-1})**			
[NMBZA]	**[MePhOH]**	**Genosorb-1843**	**295.15**	**308.15**	**328.15**	**353.15**

0.72	0.78	3.07	9.37E-11	1.35E-10	2.29E-10	3.38E-10
1.07	1.20	2.72	7.82E-11	1.26E-10	1.94E-10	3.09E-10
1.32	1.48	2.47	5.86E-11	9.50E-11	1.55E-10	2.87E-10
1.79	1.98	2.03	3.84E-11	7.82E-11	1.38E-10	2.53E-10
2.23	2.48	1.61	3.34E-11	5.51E-11	1.08E-10	2.24E-10
2.78	3.11	1.07	1.77E-11	3.66E-11	8.62E-11	2.00E-10
3.50	3.88	0.39	8.80E-12	2.24E-11	6.00E-11	1.85E-10

Concentration (kmol.m^{-3})			**Henry's constant of CO_2 in NMBZA (kPa.m^3.kmol^{-1})**			
[NMBZA]	**[MePhOH]**	**Genosorb-1843**	**295.15**	**308.15**	**328.15**	**353.15**
0.72	0.78	3.07	9.37E-11	1.35E-10	2.29E-10	3.38E-10
1.07	1.20	2.72	7.82E-11	1.26E-10	1.94E-10	3.09E-10
1.32	1.48	2.47	5.86E-11	9.50E-11	1.55E-10	2.87E-10
1.79	1.98	2.03	3.84E-11	7.82E-11	1.38E-10	2.53E-10
2.23	2.48	1.61	3.34E-11	5.51E-11	1.08E-10	2.24E-10
2.78	3.11	1.07	1.77E-11	3.66E-11	8.62E-11	2.00E-10
3.50	3.88	0.39	8.80E-12	2.24E-11	6.00E-11	1.85E-10

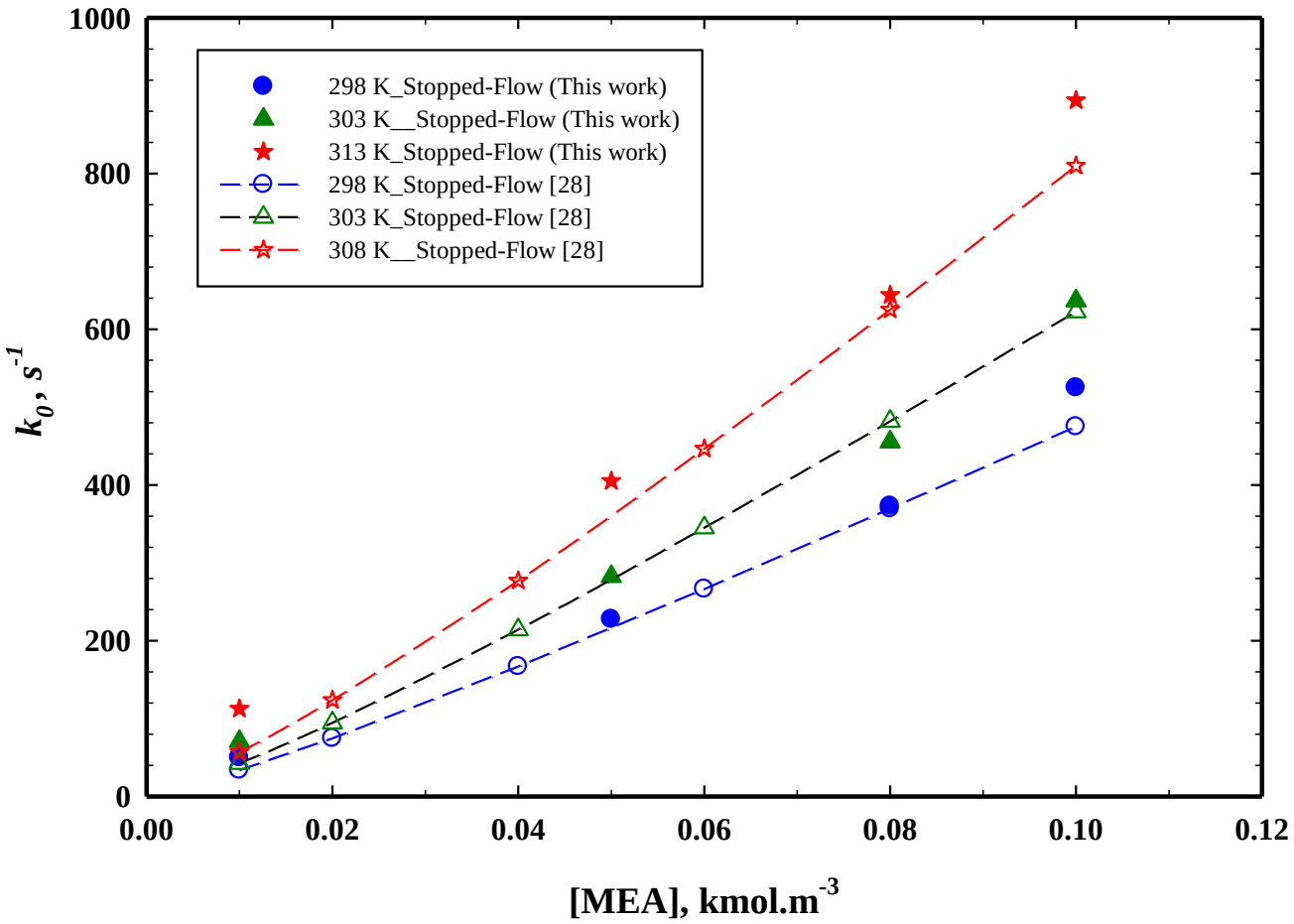

Figure 12. Comparison of measured reaction kinetics of aqueous MEA with CO_2 (hydrophilic system) using stopped-flow equipment at low concentrations with literature [28]

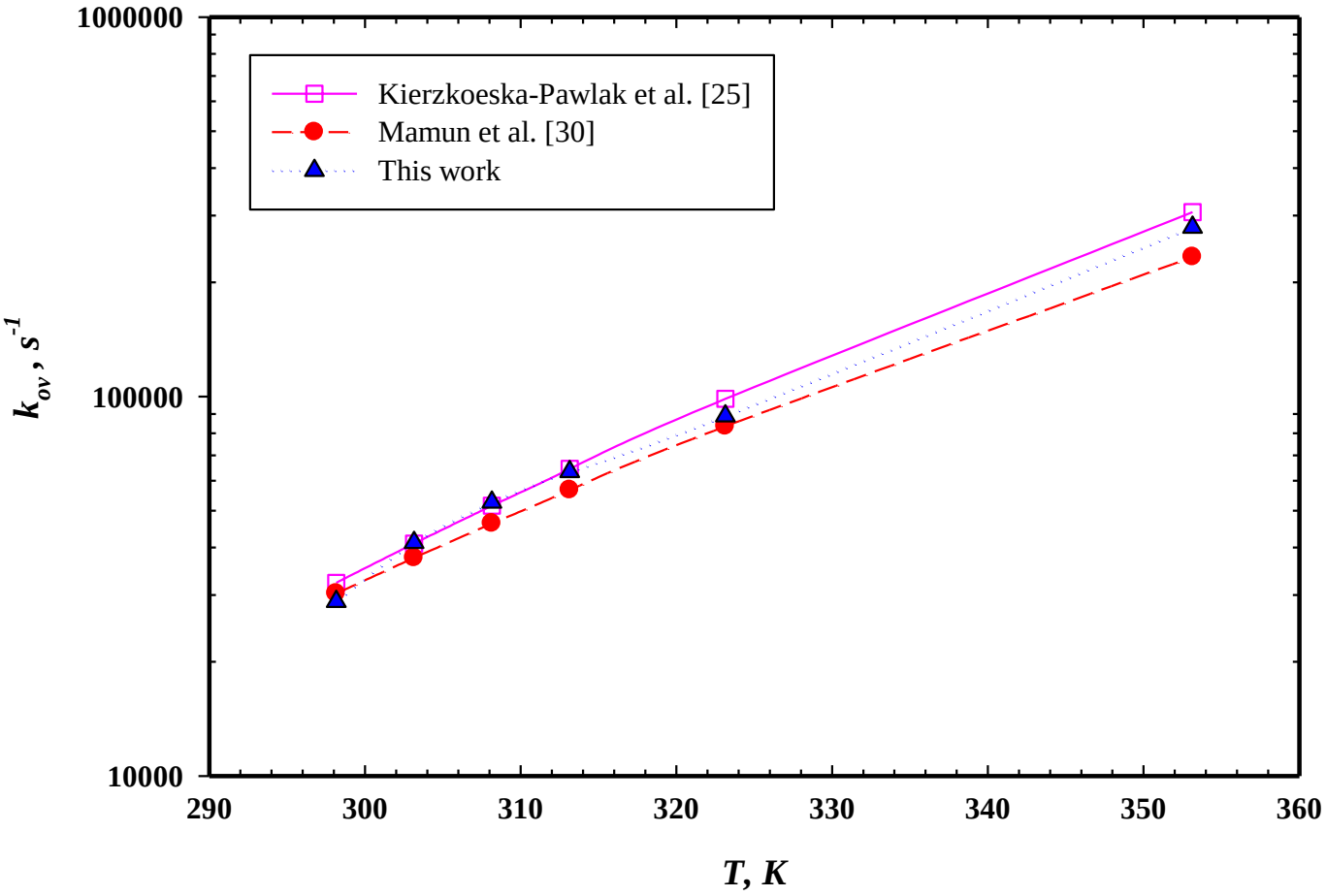

Figure 13. Measured reaction kinetics of aqueous AEEA with CO_2 (hydrophilic system) using Stirred-tank reactor compared with literature [25, 30]

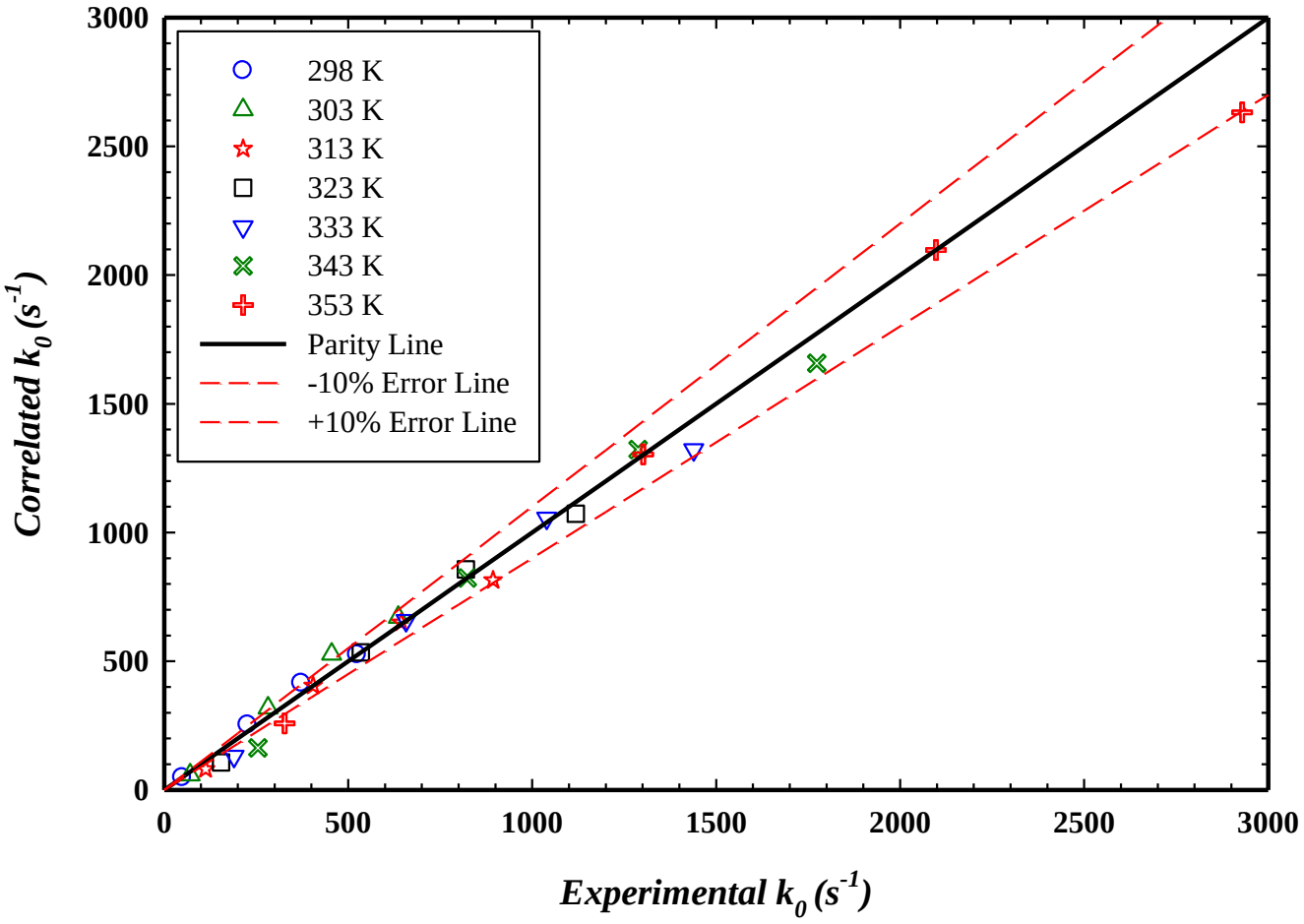

Figure 14. Parity plot for MEA

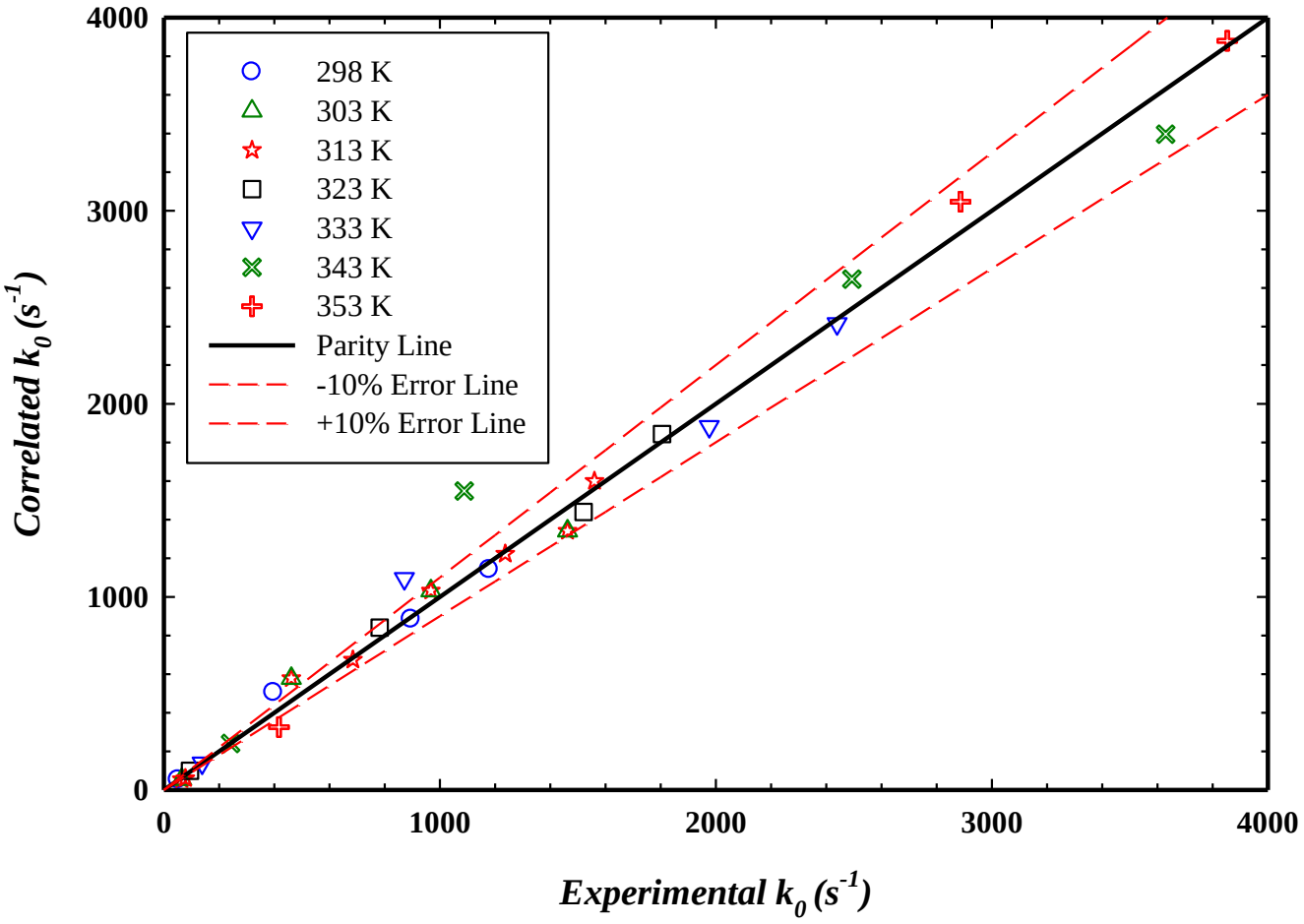

Figure 15. Parity plot for NMBZA

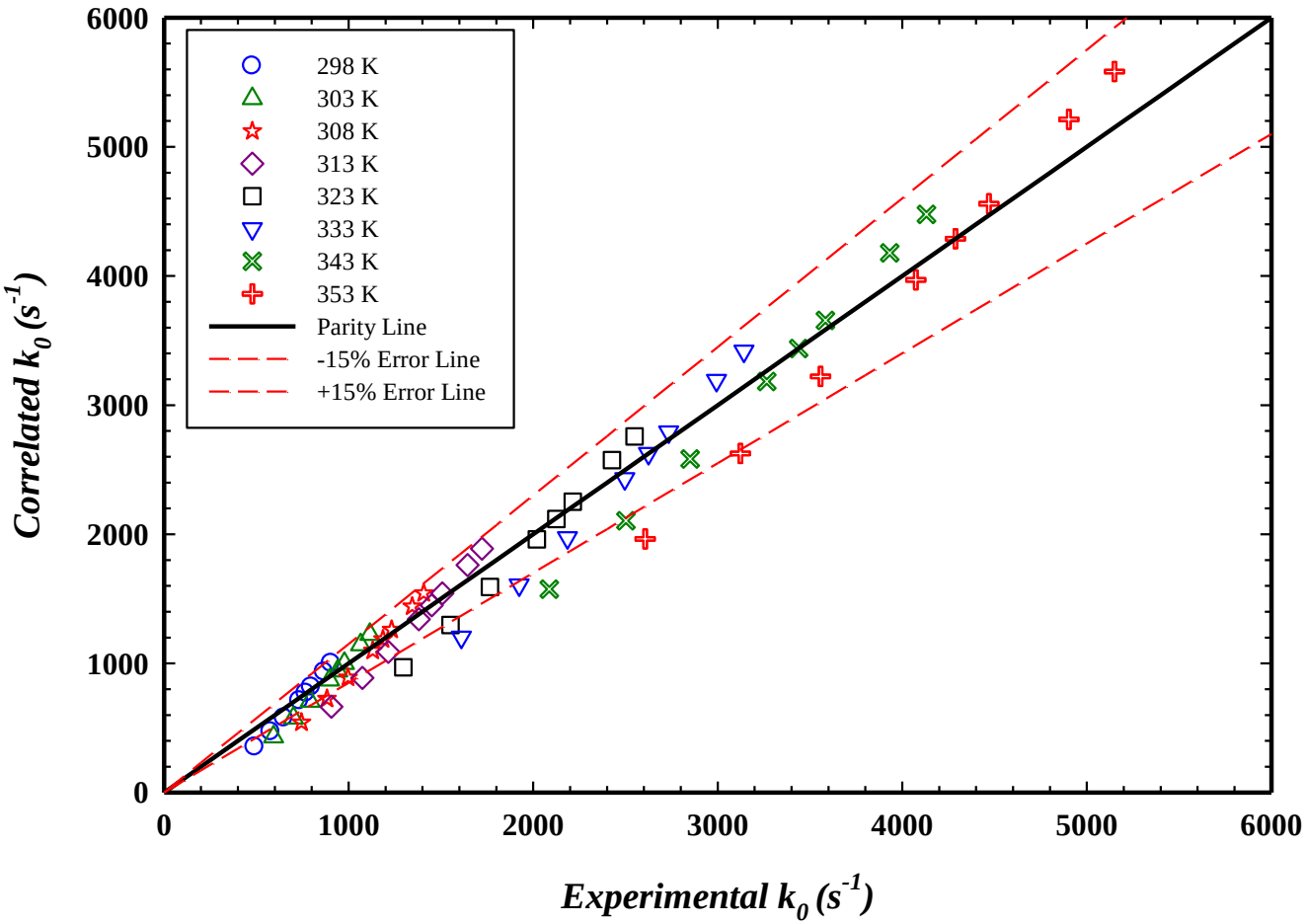

Figure 16. Parity plot for NMBZA + TEGDBE

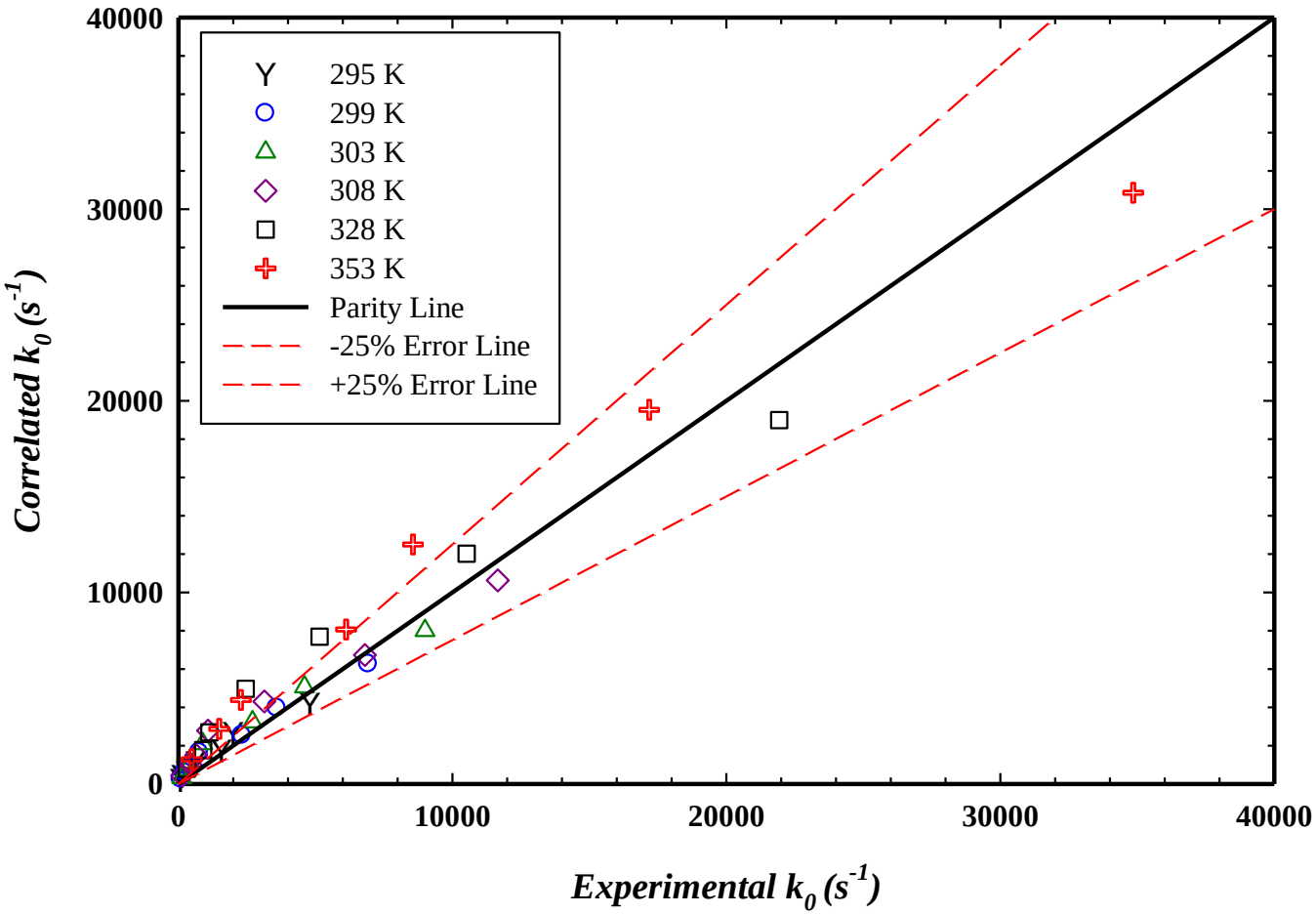

Figure 17. Parity plot for NMBZA + MePhOH + Genosorb 1843

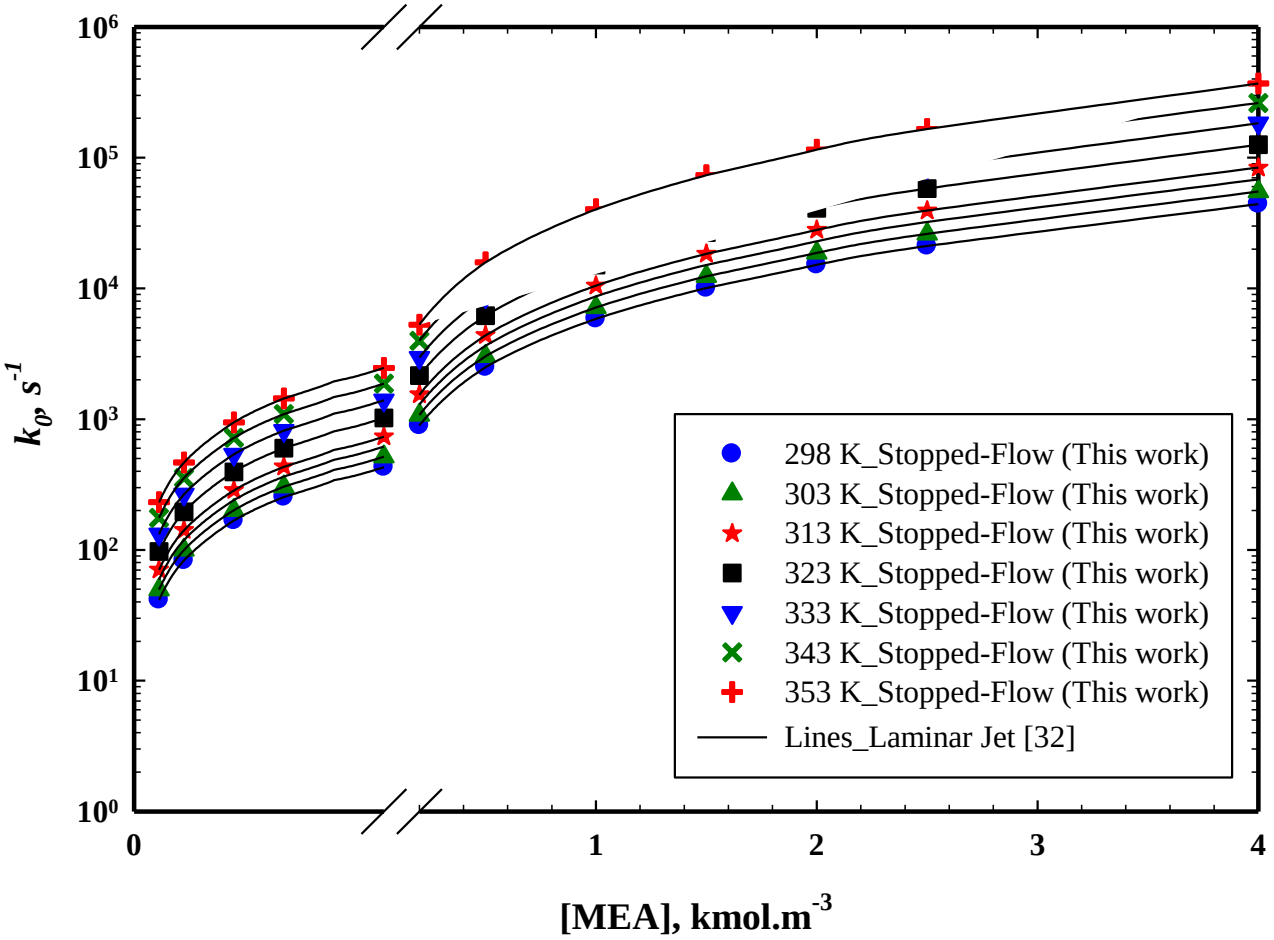

Figure 18. Predicted reaction kinetics of aqueous MEA with CO_2 from low to higher concentrations using zwitterionic model

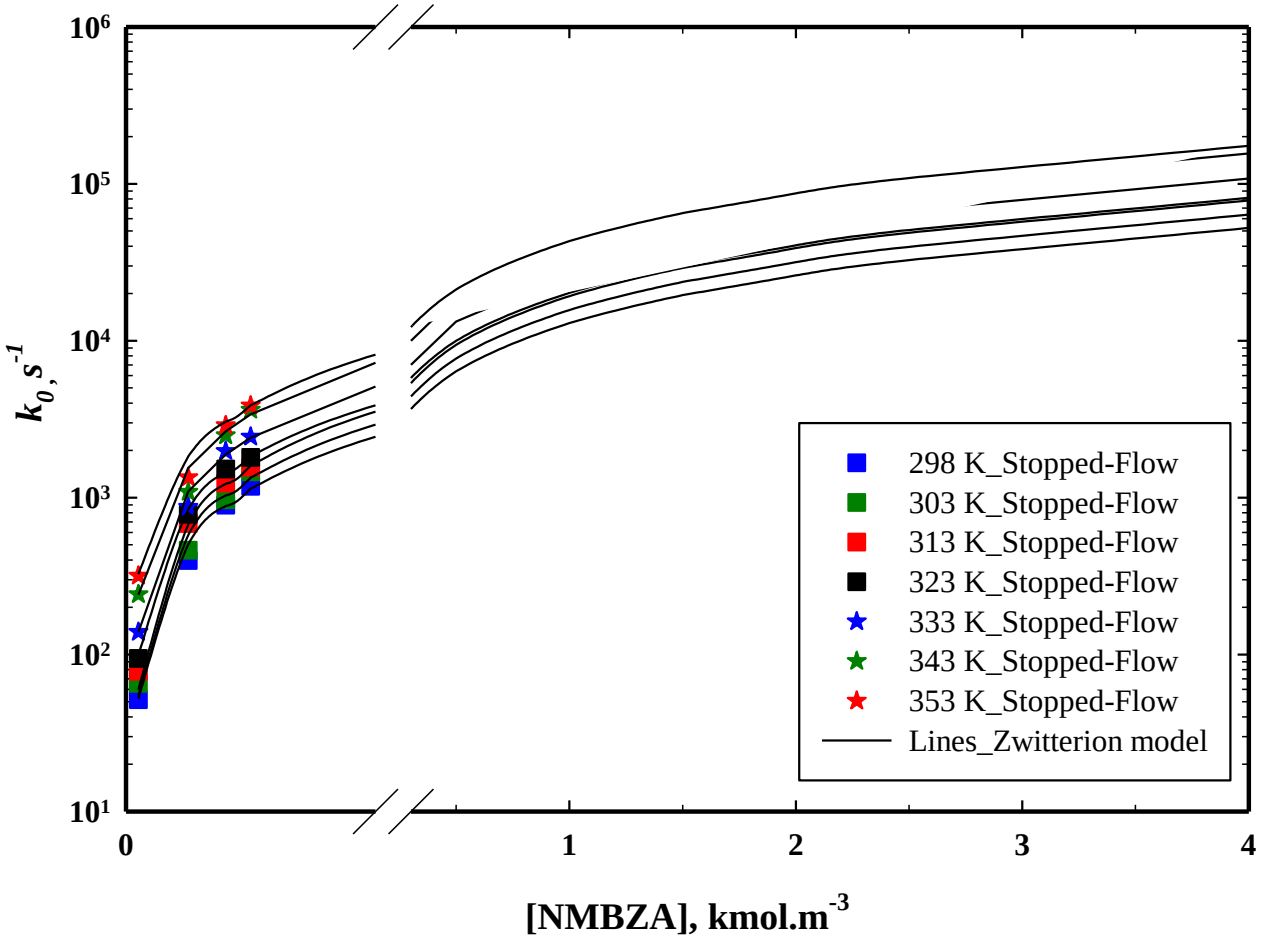

Figure 19. Predicted reaction kinetics of aqueous NMBZA with CO_2 from low to higher concentrations using zwitterionic model

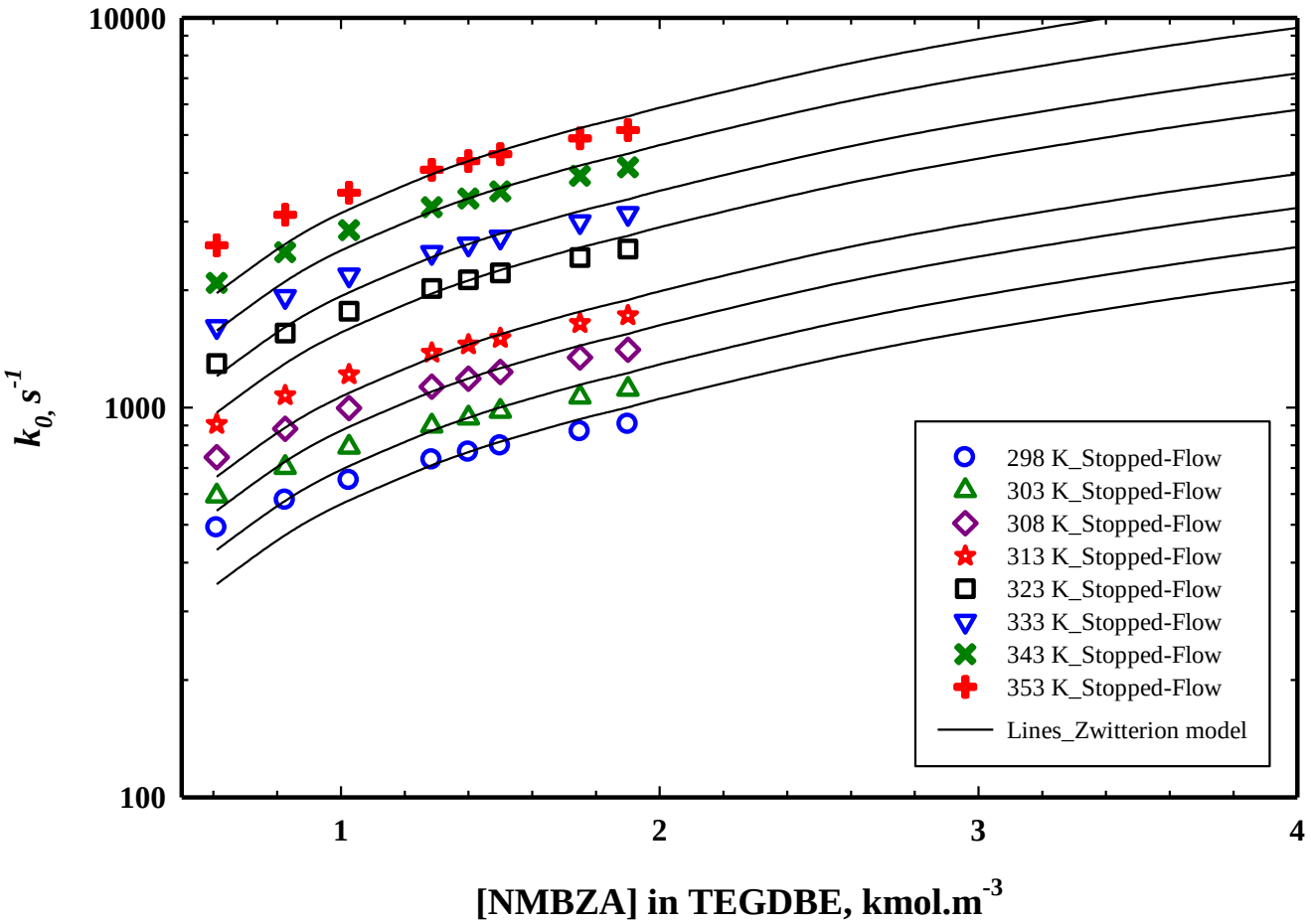

Figure 20. Predicted reaction kinetics of NMBZA + TEGDBE with CO_2 from low to higher concentrations using Zwitterionic model

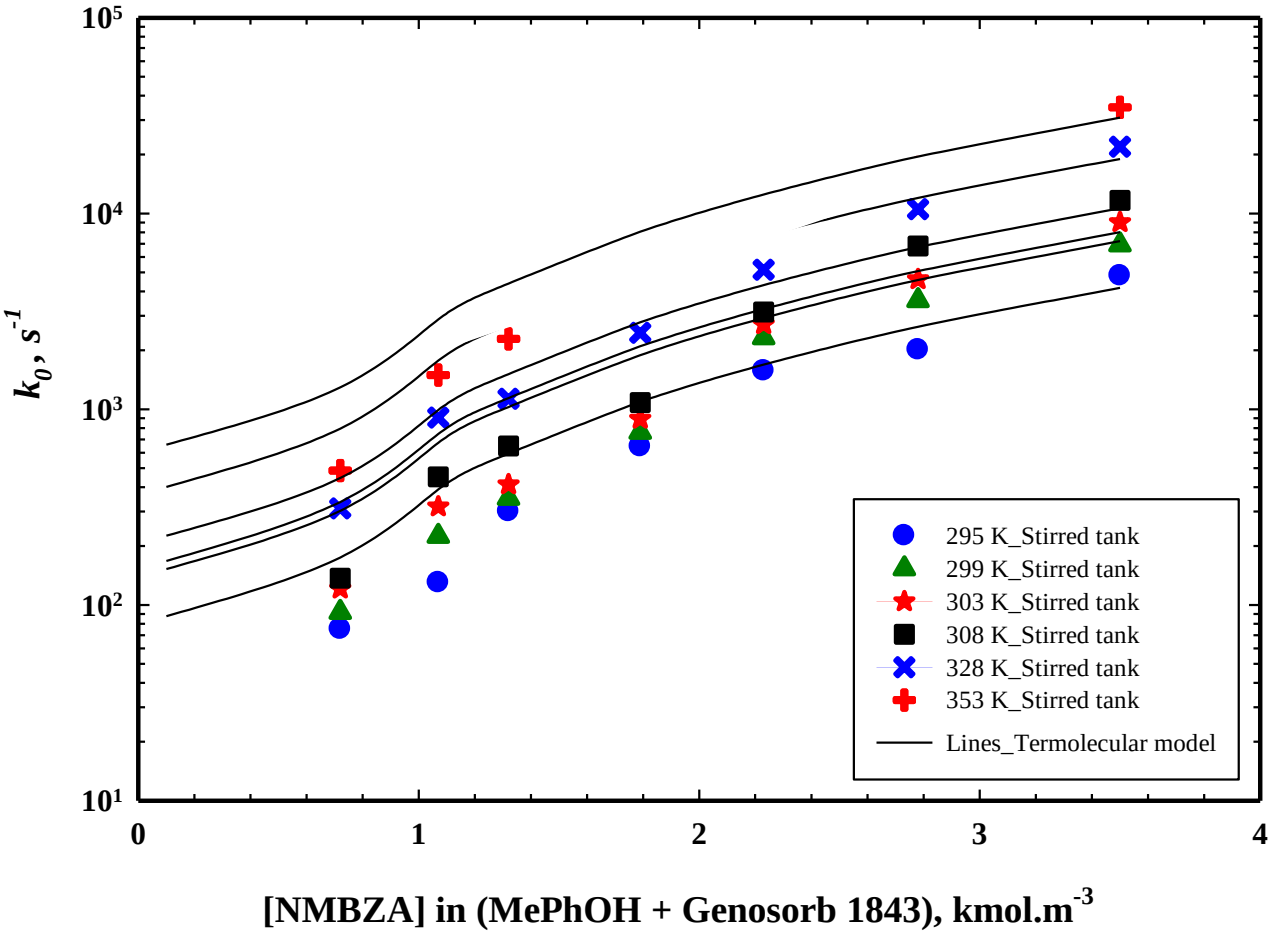

Figure 21. Predicted reaction kinetics of non-aqueous NMBZA (MePhOH + Genosorb 1843) with CO_2 from high to lower concentrations using termolecular model

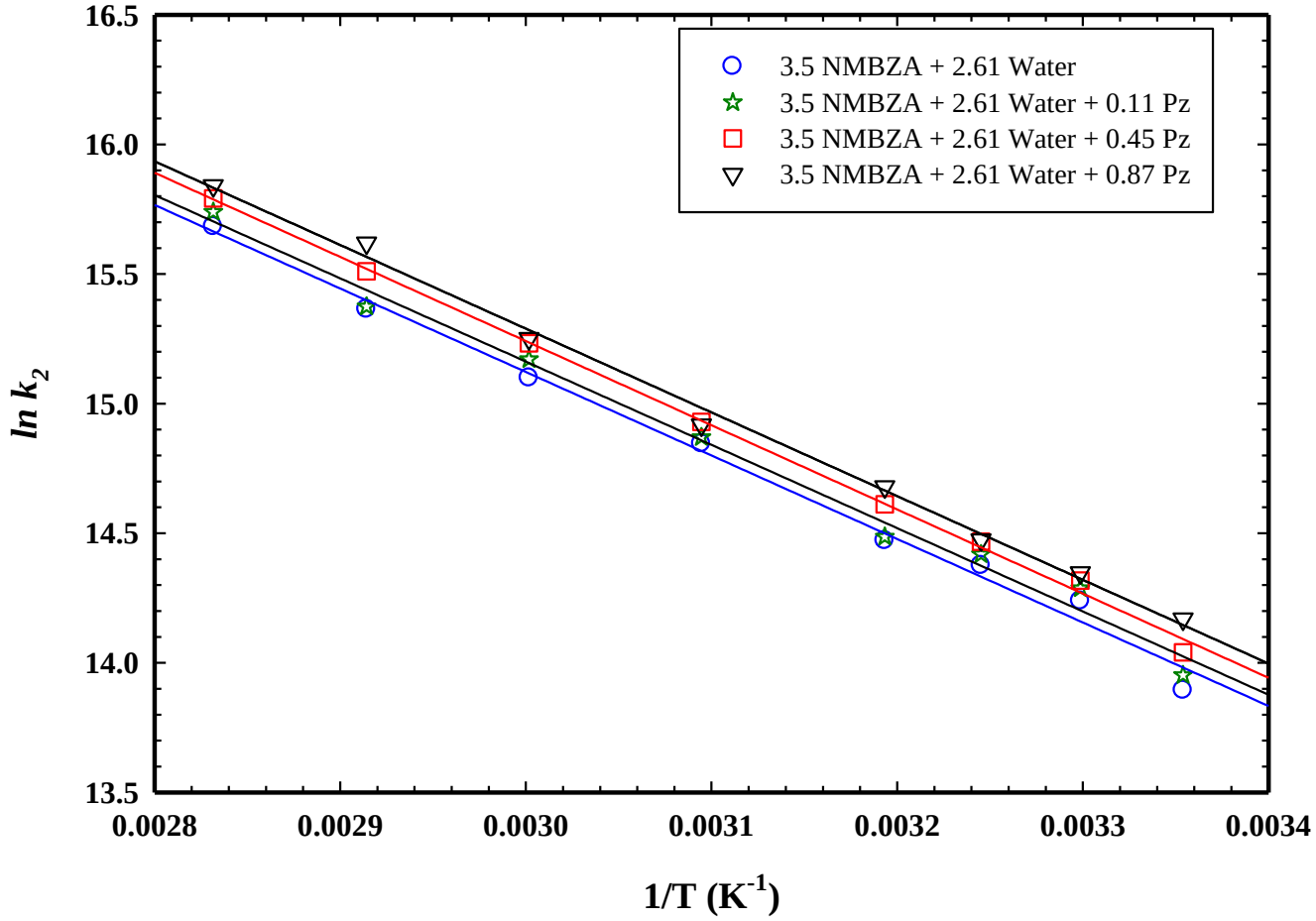

Figure 22. Comparison of second-order reaction rate constants of CO_2 with mixture of NMBZA + TEGDBE (hydrophobic system) with different concentrations of Pz at different temperatures. Lines are Arrhenius equation fits using Equation 22.

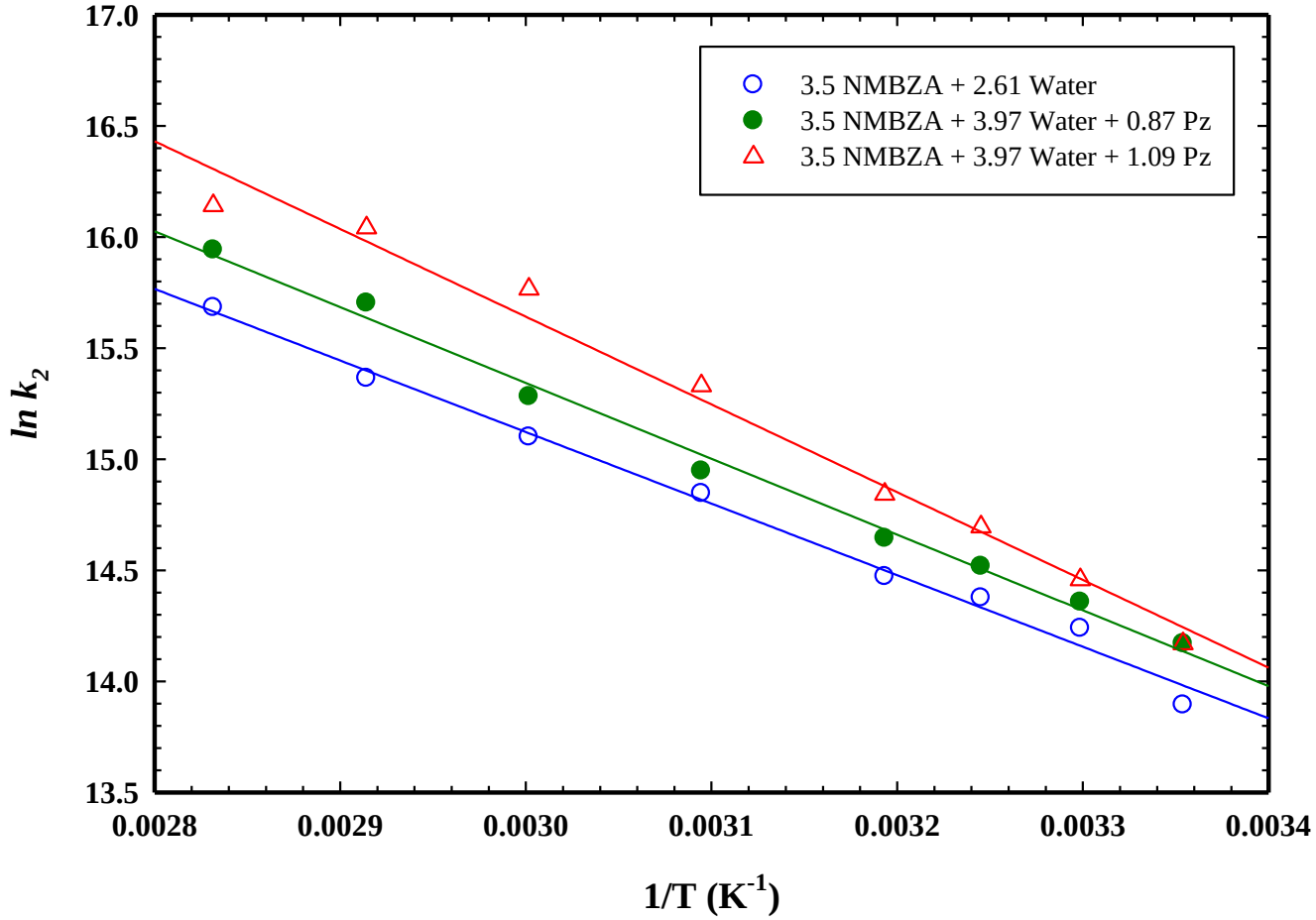

Figure 23. Comparison of second-order reaction rate constants of CO_2 with mixture of NMBZA + TEGDBE (hydrophobic system) with different concentrations of water and Pz at different temperatures. Lines are Arrhenius equation fits using Equation 22.

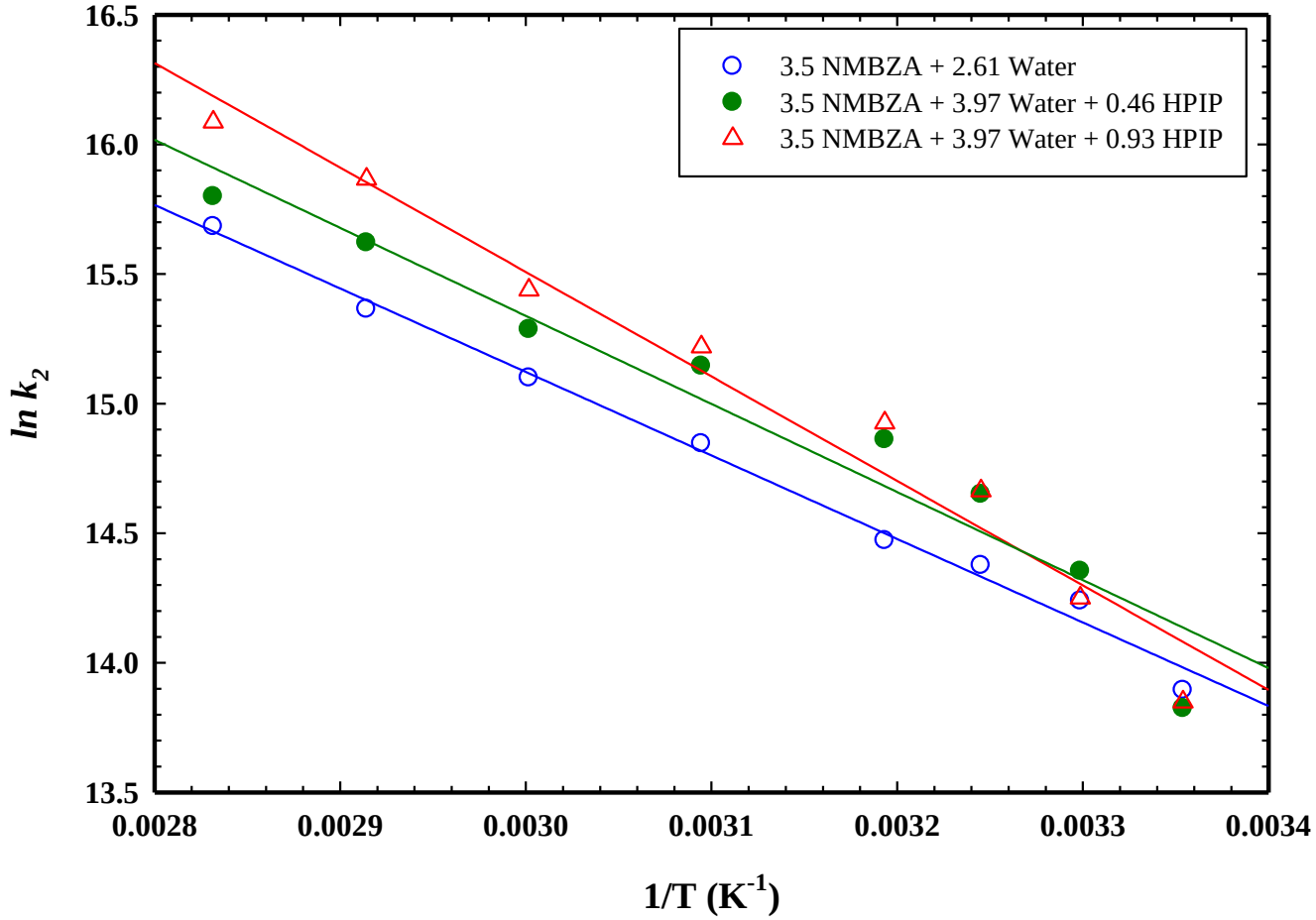

Figure 24. Comparison of second-order reaction rate constants of CO_2 with mixture of NMBZA + TEGDBE (hydrophobic system) with different concentrations of water and HPIP at different temperatures. Lines are Arrhenius equation fits using Equation 22.

References

[1] G.T. Rochelle, Amine Scrubbing for CO2 Capture, Science 325 (2009) 1652-1654.

[2] J. Oexmann, A. Kather, Minimising the regeneration heat duty of post-combustion CO2 capture by wet chemical absorption: The misguided focus on low heat of absorption solvents, International Journal of Greenhouse Gas Control 4 (2010) 36-43.

[3] P.D. Mobley, A.V. Rayer, J. Tanthana, T.R. Gohndrone, M. Soukri, L.J.I. Coleman, M. Lail, CO2 Capture Using Fluorinated Hydrophobic Solvents, Industrial & Engineering Chemistry Research 56 (2017) 11958-11966.

[4] M. Wang, A. Lawal, P. Stephenson, J. Sidders, C. Ramshaw, Post-combustion CO2 capture with chemical absorption: A state-of-the-art review, Chemical Engineering Research and Design 89 (2011) 1609-1624.

[5] M. Lail, J. Tanthana, L. Coleman, Non-Aqueous Solvent (NAS) CO2 Capture Process, Energy Procedia 63 (2014) 580-594.

[6] A.V. Rayer, A. Henni, J. Li, Reaction kinetics of 2-((2-aminoethyl) amino) ethanol in aqueous and non-aqueous solutions using the stopped-flow technique, The Canadian Journal of Chemical Engineering 91 (2013) 490-498.

[7] M.C. Lail, L., Regenerable Solvent mixtures for Acid-Gas separation., in: R. International (Ed.), 2011.

[8] D.J. Heldebrant, C.R. Yonker, P.G. Jessop, L. Phan, CO2 -binding organic liquids (CO2 BOLs) for post-combustion CO2 capture, Energy Procedia 1 (2009) 1187-1195.

[9] M.C. Ozturk, O. Yuksel Orhan, E. Alper, Kinetics of carbon dioxide binding by 1,1,3,3-tetramethylguanidine in 1-hexanol, International Journal of Greenhouse Gas Control 26 (2014) 76-82.

[10] F.P. Gordesli, C.S. Ume, E. Alper, Mechanism and Kinetics of Carbon Dioxide Capture Using Activated 2-Amino-2-methyl-1,3-propanediol, International Journal of Chemical Kinetics 45 (2013) 566-573.

[11] M.C. Öztürk, The Reaction Mechanism and Kinetics of Carbon Dioxide Binding Organic Liquids, Hacettepe University,Ankara, 2011.

[12] O. Yuksel Orhan, The Absorption Kinetics of CO2 into Ionic-Liquid-CO2 Binding Organic Liquid Hybrid Solevents, Hacettepe University, 2014.

[13] P.V. Kortunov, M. Siskin, L.S. Baugh, D.C. Calabro, In Situ Nuclear Magnetic Resonance Mechanistic Studies of Carbon Dioxide Reactions with Liquid Amines in Non-aqueous Systems: Evidence for the Formation of Carbamic Acids and Zwitterionic Species, Energy & Fuels 29 (2015) 5940-5966.

[14] R.J. Perry, M.J. O'Brien, Amino Disiloxanes for CO2 Capture, Energy & Fuels 25 (2011) 1906-1918.

[15] L. Heuer, Benzylamine, Wiley-VCH Verlag GmbH & Co. KGaA, Weingeim2000.

[16] S. Martin, H. Lepaumier, D. Picq, J. Kittel, T. de Bruin, A. Faraj, P.-L. Carrette, New Amines for CO2 Capture. IV. Degradation, Corrosion, and Quantitative Structure Property Relationship Model, Industrial & Engineering Chemistry Research 51 (2012) 6283-6289.

[17] J.B. Matthews, J.F. Sumner, E.A. Moelwyn-Hughes, The vapour pressures of certain liquids, Transactions of the Faraday Society 46 (1950) 797-803.

[18] I. Mokbel, A. Razzouk, T. Sawaya, J. Jose, Experimental Vapor Pressures of 2-Phenylethylamine, Benzylamine, Triethylamine, and cis-2,6-Dimethylpiperidine in the Range between 0.2 Pa and 75 kPa, Journal of Chemical & Engineering Data 54 (2009) 819-822.

[19] G. Richner, G. Puxty, A. Carnal, W. Conway, M. Maeder, P. Pearson, Thermokinetic properties and performance evaluation of benzylamine-based solvents for CO2 capture, Chemical Engineering Journal 264 (2015) 230-240.

[20] P.G. Jessop, C.A. Eckert, C.L. Liotta, D.J. Heldebrant, Switchable solvents and methods of use thereof, Google Patents, 2014.

[21] O. Yuksel Orhan, E. Alper, Kinetics of reaction between CO2 and ionic liquid-carbon dioxide binding organic liquid hybrid systems: Analysis of gas-liquid absorption and stopped flow experiments, Chemical Engineering Science 170 (2017) 36-47.

[22] M. Caplow, Kinetics of carbamate formation and breakdown, Journal of the American Chemical Society 90 (1968) 6795-6803.

[23] P.V. Danckwerts, The reaction of CO2 with ethanolamines, Chemical Engineering Science 34 (1979) 443-446.

[24] J.E. Crooks, J.P. Donnellan, Kinetics and mechanism of the reaction between carbon dioxide and amines in aqueous solution, Journal of the Chemical Society, Perkin Transactions 2 (1989) 331-333.

[25] H. Kierzkowska-Pawlak, A. Chacuk, M. Siemieniec, Reaction kinetics of CO2 in aqueous 2-(2-aminoethylamino)ethanol solutions using a stirred cell reactor, International Journal of Greenhouse Gas Control 24 (2014) 106-114.

[26] Clariant, Genosorb 1843-Absorption Fluid.

[27] A.C. Knipe, D. McLean, R.L. Tranter, A fast response conductivity amplifier for chemical kinetics, Journal of Physics E: Scientific Instruments 7 (1974) 586.

[28] S.H. Ali, Kinetics of the reaction of carbon dioxide with blends of amines in aqueous media using the stopped-flow technique, International Journal of Chemical Kinetics 37 (2005) 391-405.

[29] C.R. Wilke, P. Chang, Correlation of diffusion coefficients in dilute solutions, AIChE Journal 1 (1955) 264-270.

[30] S. Ma'mun, V.Y. Dindore, H.F. Svendsen, Kinetics of the Reaction of Carbon Dioxide with Aqueous Solutions of 2-((2-Aminoethyl)amino)ethanol, Industrial & Engineering Chemistry Research 46 (2007) 385-394.

[31] F. Leder, The absorption of CO2 into chemically reactive solutions at high temperatures, Chemical Engineering Science 26 (1971) 1381-1390.

[32] A. Aboudheir, P. Tontiwachwuthikul, A. Chakma, R. Idem, Kinetics of the reactive absorption of carbon dioxide in high CO2-loaded, concentrated aqueous monoethanolamine solutions, Chemical Engineering Science 58 (2003) 5195-5210.

[33] J. Li, A. Henni, P. Tontiwachwuthikul, Reaction Kinetics of CO2 in Aqueous Ethylenediamine, Ethyl Ethanolamine, and Diethyl Monoethanolamine Solutions in the

Temperature Range of 298−313 K, Using the Stopped-Flow Technique, Industrial & Engineering Chemistry Research 46 (2007) 4426-4434.

[34] A.V. Rayer, K.Z. Sumon, A. Henni, P. Tontiwachwuthikul, Kinetics of the reaction of carbon dioxide (CO2) with cyclic amines using the stopped-flow technique, Energy Procedia 4 (2011) 140-147.

[35] R.A. Davis, O.C. Sandall, Kinetics of the reaction of carbon dioxide with secondary amines in polyethylene glycol, Chemical Engineering Science 48 (1993) 3187-3193.

[36] S. Kadiwala, A.V. Rayer, A. Henni, Kinetics of carbon dioxide (CO2) with ethylenediamine, 3-amino-1-propanol in methanol and ethanol, and with 1-dimethylamino-2-propanol and 3-dimethylamino-1-propanol in water using stopped-flow technique, Chemical Engineering Journal 179 (2012) 262-271.

[37] F.P.G. Duatepe, E. Alper, Reaction Kinetics of Carbon Dioxide with Nonaqueous Solutions of Sterically Hindered Amines, (2016).

[38] E. Sada, H. Kumazawa, Z.Q. Han, H. Matsuyama, Chemical kinetics of the reaction of carbon dioxide with ethanolamines in nonaqueous solvents, AIChE Journal 31 (1985) 1297-1303.

[39] E. Sada, H. Kumazawa, Y. Ikehara, Z.Q. Han, Chemical kinetics of the reaction of carbon dioxide with triethanolamine in non-aqueous solvents, The Chemical Engineering Journal 40 (1989) 7-12.

[40] E. Sada, H. Kumazawa, Y. Osawa, M. Matsuura, Z.Q. Han, Reaction kinetics of carbon dioxide with amines in non-aqueous solvents, The Chemical Engineering Journal 33 (1986) 87-95.

[41] G.F. Versteeg, W.P.M. van Swaaij, On the kinetics between CO2 and alkanolamines both in aqueous and non-aqueous solutions—II. Tertiary amines, Chemical Engineering Science 43 (1988) 587-591.

[42] S.-W. Park, B.-S. Choi, J.-W. Lee, Chemical absorption of carbon dioxide with triethanolamine in non-aqueous solutions, Korean Journal of Chemical Engineering 23 (2006) 138-143.

[43] S.-W. Park, J.-W. Lee, B.-S. Choi, J.-W. Lee, Absorption of carbon dioxide into non-aqueous solutions ofN-methyldiethanolamine, Korean Journal of Chemical Engineering 23 (2006) 806-811.

[44] S.H. Ali, S.Q. Merchant, M.A. Fahim, Kinetic study of reactive absorption of some primary amines with carbon dioxide in ethanol solution, Separation and Purification Technology 18 (2000) 163-175.

[45] J. Li, T.U.o.R. . Kinetic Study of Carbon Dioxide and Alkanolamines Both in Aqueous and Non-aqueous Solutions Using the Stopped Flow Technique, University of Regina (Canada)2007.

[46] M.Ç. Öztürk, C.S. Ume, E. Alper, Reaction Mechanism and Kinetics of 1,8-Diazabicyclo[5.4.0]undec-7-ene and Carbon Dioxide in Alkanol Solutions, Chemical Engineering & Technology 35 (2012) 2093-2098.

[47] P.M. Mathias, F. Zheng, D.J. Heldebrant, A. Zwoster, G. Whyatt, C.M. Freeman, M.D. Bearden, P. Koech, Measuring the Absorption Rate of CO2 in Nonaqueous CO2-Binding Organic Liquid Solvents with a Wetted-Wall Apparatus, ChemSusChem 8 (2015) 3617-3625.

[48] G.A. Whyatt, C.J. Freeman, A. Zwoster, D.J. Heldebrant, Measuring Nitrous Oxide Mass Transfer into Non-Aqueous CO2BOL CO2 Capture Solvents, Industrial & Engineering Chemistry Research 55 (2016) 4720-4725.

[49] D.J. Heldebrant, P.G. Jessop, C.A. Thomas, C.A. Eckert, C.L. Liotta, The Reaction of 1,8-Diazabicyclo[5.4.0]undec-7-ene (DBU) with Carbon Dioxide, The Journal of Organic Chemistry 70 (2005) 5335-5338.

[50] G. Astarita, Carbon dioxide absorption in aqueous monoethanolamine solutions, Chemical Engineering Science 16 (1961) 202-207.

[51] R.E. Emmert, R.L. Pigford, Gas absorption accompanied by chemical reaction: A study of the absorption of carbon dioxide in aqueous solutions of monoethanolamine, AIChE Journal 8 (1962) 171-175.

[52] J.K.A. Clarke, Kinetics of Absorption of Cardon Dioxide in Monoethanolamine Solutions at Short Contact Times, Industrial & Engineering Chemistry Fundamentals 3 (1964) 239-245.

[53] M.M. Sharma, Kinetics of reactions of carbonyl sulphide and carbon dioxide with amines and catalysis by Bronsted bases of the hydrolysis of COS, Transactions of the Faraday Society 61 (1965) 681-688.

[54] P.V. Danckwerts, M.M. Sharma, The absorption of carbon dioxide into solutions of alkalis and amines : (with some notes on hydrogen sulphide and carbonyl sulphide), Institution of Chemical Engineers, London, 1966.

[55] E. Sada, H. Kumazawa, M.A. Butt, Gas absorption with consecutive chemical reaction: Absorption of carbon dioxide into aqueous amine solutions, The Canadian Journal of Chemical Engineering 54 (1976) 421-424.

[56] E. Sada, H. Kumazawa, M.A. Butt, D. Hayashi, Simultaneous absorption of carbon dioxide and hydrogen sulfide into aqueous monoethanolamine solutions, Chemical Engineering Science 31 (1976) 839-841.

[57] E. Sada, H. Kumazawa, M.A. Butt, J.E. Lozano, Interfacial turbulence accompanying chemical absorption, The Canadian Journal of Chemical Engineering 55 (1977) 293-296.

[58] H. Hikita, S. Asai, H. Ishikawa, M. Honda, The kinetics of reactions of carbon dioxide with monoethanolamine, diethanolamine and triethanolamine by a rapid mixing method, The Chemical Engineering Journal 13 (1977) 7-12.

[59] H. Hikita, S. Asai, Y. Katsu, S. Ikuno, Absorption of carbon dioxide into aqueous monoethanolamine solutions, AIChE Journal 25 (1979) 793-800.

[60] C. Alvarez-Fuster, N. Midoux, A. Laurent, J.C. Charpentier, Chemical kinetics of the reaction of carbon dioxide with amines in pseudo m-nth order conditions in aqueous and organic Solutions, Chemical Engineering Science 35 (1980) 1717-1723.

[61] T.L. Donaldson, Y.N. Nguyen, Carbon Dioxide Reaction Kinetics and Transport in Aqueous Amine Membranes, Industrial & Engineering Chemistry Fundamentals 19 (1980) 260-266.

[62] S.S. Laddha, P.V. Danckwerts, Reaction of CO2 with ethanolamines: kinetics from gas-absorption, Chemical Engineering Science 36 (1981) 479-482.

[63] D.E. Penny, T.J. Ritter, Kinetic study of the reaction between carbon dioxide and primary amines, Journal of the Chemical Society, Faraday Transactions 1: Physical Chemistry in Condensed Phases 79 (1983) 2103-2109.

[64] D. Barth, C. Tondre, J.J. Delpuech, Stopped-flow investigations of the reaction kinetics of carbon dioxide with some primary and secondary alkanolamines in aqueous solutions, International Journal of Chemical Kinetics 18 (1986) 445-457.

[65] E. Alper, Reaction mechanism and kinetics of aqueous solutions of 2-amino-2-methyl-1-propanol and carbon dioxide, Industrial & Engineering Chemistry Research 29 (1990) 1725-1728.

[66] R.J. Littel, G.F. Versteeg, W.P.M. Van Swaaij, Kinetics of CO2 with primary and secondary amines in aqueous solutions—II. Influence of temperature on zwitterion formation and deprotonation rates, Chemical Engineering Science 47 (1992) 2037-2045.

[67] D.P. Hagewiesche, S.S. Ashour, H.A. Al-Ghawas, O.C. Sandall, Absorption of carbon dioxide into aqueous blends of monoethanolamine and N-methyldiethanolamine, Chemical Engineering Science 50 (1995) 1071-1079.

[68] J. Xiao, C.-W. Li, M.-H. Li, Kinetics of absorption of carbon dioxide into aqueous solutions of 2-amino-2-methyl-1-propanol+monoethanolamine, Chemical Engineering Science 55 (2000) 161-175.

[69] S.-Y. Horng, M.-H. Li, Kinetics of Absorption of Carbon Dioxide into Aqueous Solutions of Monoethanolamine + Triethanolamine, Industrial & Engineering Chemistry Research 41 (2002) 257-266.

[70] M. Edali, A. Aboudheir, R. Idem, Kinetics of carbon dioxide absorption into mixed aqueous solutions of MDEA and MEA using a laminar jet apparatus and a numerically solved 2D absorption rate/kinetics model, International Journal of Greenhouse Gas Control 3 (2009) 550-560.

[71] W. Conway, X. Wang, D. Fernandes, R. Burns, G. Lawrance, G. Puxty, M. Maeder, Comprehensive Kinetic and Thermodynamic Study of the Reactions of CO2(aq) and HCO3–

with Monoethanolamine (MEA) in Aqueous Solution, The Journal of Physical Chemistry A 115 (2011) 14340-14349.